

HOUSE RESPONSE FROM BLAST-INDUCED LOW FREQUENCY GROUND VIBRATIONS AND INSPECTIONS FOR RELATED INTERIOR CRACKING

Final Report to the Office of Surface Mining
Contract ID: 143868-PO96-12616

Produced by:

Steven V. Crum¹
Geophysicist

S-Wave GeoTech
5016 Russell Avenue South
Minneapolis, Minnesota 55410

July 14, 1997

"This report is based upon work funded by the Office of Surface Mining Reclamation and Enforcement. The views and conclusions contained in this document are solely those of the author/s and should not be interpreted as necessarily representing the official policies or recommendations of the U.S. Department of the Interior, Office of Surface Mining Reclamation and Enforcement, or of the United States Government."

Previously with the former U. S. Bureau of Mines, Twin Cities Research Center, Minneapolis, MN.

TABLE OF CONTENTS

Abstract	1
Introduction	2
Principal Structural Monitoring	2
Causes and Classification of Structural Cracking	3
Differential Displacement and Strain	3
House Response	5
Natural Frequency	6
Amplification	6
Damping	7
Quasi-Free Vibration	7
Ground Vibrations and Structure Response	8
Test Homes	8
Monitoring	9
Observations Based on Full-Waveform Recordings	10
Response to Natural Frequency Excitation	10
Response to High Frequency Excitation	11
Response to Low Frequency Excitation	11
Effects of Ground Vibration Duration on Structure Response	11
Natural Frequencies of the Test Homes	12
Structural Amplification of Ground Vibration	14
Data Reduction	15
Results	16
Response Velocity vs. Ground Vibration Velocity	17
Observations of Blast-Induced Cracking	18
Procedure	18
Results of the Crack Investigations	19
Airblast	20
Conclusions	21
Acknowledgments	22
References	23
Tables	25
Figures	27 - 52
Appendix A: Data Tables	A-0 thru A-5
Appendix B: Selected Ground Vibration and Response Recordings	B-0 thru B-20

ABSTRACT

This study was initiated in response to concerns expressed by citizen's groups, regulatory authorities and the former Bureau of Mines, that current regulatory guidelines for low frequency ground vibrations were insufficient to protect homes from cracking and damage. The study was originally directed to examine the response of structures to low frequency ground vibrations; defined as frequencies below the structural natural frequency. Early in the investigation, however, researchers found that the occurrence of low frequency ground vibrations with the potential to cause cracking in homes was quite rare. The study was subsequently expanded to include a broader range of frequencies but retained the original focus to measure house response motions from blast vibrations and inspect for vibrations-related cracking.

Ten different homes at five separate blasting operations were incorporated in the study providing a variety of structural types and locations. Ground vibration and structure response recordings were made from over 170 blasts with a range of maximum ground vibration amplitudes from 0.04 to 6.0 in/s. The frequencies associated with maximum horizontal ground vibration velocities spanned from about 2.5 to 70 Hz, equating to about 1/2- to 6-times the natural frequencies of the structures studied. The largest structural response amplifications of 3- to 5-times the ground motion were produced from ground vibrations with dominant frequencies from about 0.9 to 2-times the structural natural frequency, in general agreement with other published findings. Lower maximum response amplifications were generated from ground vibrations with dominant frequencies outside of this frequency range.

Structural amplifications from low frequency ground vibrations were comparable to or less than structural amplifications from higher frequencies. This indicates that low frequency ground vibrations from blasting do not have an increased risk of inducing cosmetic cracking in homes compared to higher frequency ground vibrations and may even pose less of a threat than the worse-case condition of ground vibration excitation frequencies at the structural natural frequency. These results are in agreement with structural dynamics theory.

Pre- and post-blast visual inspections for vibrations-induced cracking using 7-power optical magnifiers were made at several of the test homes. Over 350 pre- and post-blast inspections were made in relation to 46 blasts, with 22 blasts having peak ground vibration amplitudes over 1.0 in/s. Only two occurrences of vibrations-related cracking were found. Both of the instances were classified as cosmetic cracking and were associated with ground vibration amplitudes that exceeded the Bureau of Mines RI 8507 safe-level recommendations for avoiding superficial or worse forms of structural cracking in homes. The driving ground vibration is defined as the portion of the vibration time history that appeared to be causing maximum structure response.

INTRODUCTION

This report summarizes the findings from the three-year investigation by the former U. S. Bureau of Mines, Twin Cities Research Center, on the effects of blast-induced ground vibrations on low-rise residential structures. It follows three previous Bureau reports: Crum and Siskind (1993), Crum and Pierce (1994) and Pierce and Crum (1996), that describe the preliminary and intermediate findings of the investigation. Earlier Bureau of Mines reports on house response to blast-induced ground vibrations include RI 8507 (Siskind et al., 1980b) and RI 8896 (Stagg et al., 1984). RI 8485 (Siskind et al., 1980a) reported on a study of the effects of airblast on structures.

This study was undertaken in response to concerns by citizens' groups, regulatory authorities and the Bureau of Mines that the safe-level criteria established in RI 8507 (Siskind et al., 1980b) for averting vibrations-induced cracking in homes, was not adequate. It was felt that insufficient information was collected in the RI 8507 study to properly address the effects of "low-frequency" ground vibrations on homes: low frequency being defined as frequencies below the structural natural frequency. The range of natural frequencies for typical wood-frame homes is between 4 and 12 Hz (Siskind, 1980b).

The data collected in the RI 8507 study contained structure response information and cracking inspections from ground vibration with peak amplitudes from about 0.2 in/s to 10.0 in/s and frequencies from about 6 to 70 Hz. To supplement this data, the authors incorporated information published by other researchers that were not necessarily associated with mining blasts; such as structure response from earthquakes for low frequencies and construction blasts in hard rock for high frequencies. Because of likely measurement and observational inconsistencies between the various investigations, the Bureau believed it necessary to initiate a study to obtain new measurements of structure response and vibrations-induced cracking to supplement the RI 8507 findings. Because of the immediate concern over low frequency ground vibrations, emphasis was placed on studying the effects of these types of vibrations on homes.

Principal Structural Motions

There are two basic forms of motion exhibited by structures in response to ground vibration or airblast excitation: midwall and corner response. Corner response motions are indicative of whole-structure shearing, or "racking". Midwall response is essentially a flexural bending of large structural surfaces, such as walls, ceilings and floors. This type of motion is perpendicular to the plane of the surface and can be likened to the motion of a vibrating drum head. Figure 1 depicts the difference between midwall motions (bending) and shear (racking). Because cracking from blasts occur where excessive stresses and strains are produced within the planes of walls or between the walls at the corners, corner response is assumed to be a better indicator of cracking potential than midwall response (Siskind et al., 1980b, pg. 18).

Causes and Classification of Structural Cracking

Cracks form in building materials when strains exceed the material's failure level and are most often created by non-blasting causes such as settling, wood shrinkage, the influence of daily and seasonal temperature cycles, interior heating in the winter, and air conditioning in the summer. Inferior building materials and workmanship can also be responsible for material cracking (refer to Seaquist, 1980, for a thorough discussion of house structural problems). Although blast vibrations can cause structural cracking in homes, they are usually not the most likely cause².

Table 10 in RI 8507 describes a classification for cracking that is also used in this study. Threshold cracking is the first-formed and most superficial type of cracking. It involves the loosening of paint, small plaster cracks at joints between construction elements and the lengthening of old cracks. The term "threshold" pertains to the lower limit of material failure. These types of cracks are indistinguishable from naturally induced cosmetic cracks in wall coverings and do not affect structural capacities. Minor cracking is described as the loosening and falling of plaster and mortar, and cracks that are "hairline" to 3-mm in width (~0 to 1/8 in). Threshold and minor cracking are the most common forms of cracking found in homes and are often referred to as "cosmetic" because they effect only appearance and not structural integrity. Major cracking describes material failure that degrades the integrity of one or more structural components and may create general safety hazards. Examples include cracks in walls and masonry of several millimeters in width, rupture of building materials, fall of chimneys, structural weakening and permanent distortion.

Some older Bureau of Mines reports, including RI 8507, regularly use the word "damage" when referring to all forms of cracking. In the civil engineering literature, "damage" is most often associated with major cracking that impairs structural integrity and worse forms of structural failure. Regulatory manuals, however, often site "damage" as any form of cracking that decreases the value of a home. In this case, cosmetic and minor cracking may also classify as damage. This report will incorporate the traditional engineering terminology which distinguishes threshold and minor cosmetic cracking from major cracking, or "damage", that causes the degradation of structural integrity.

Differential Displacement and Strain

The basic form of the strain equation for linear deformation (i.e., lengthening or shortening) is:

$$\epsilon = \frac{\Delta L}{L} \quad (1),$$

where ϵ is strain and ΔL is the change in length, or displacement, relative to the original length L .

² A selected bibliography on this topic would include Siskind et al., 1980a, 1980b, 1993; Stagg et al., 1984; Dowding, 1985, 1996; White et al., 1993; and Crum and Pierce, 1994.

Structural engineers describe two fundamental forms of strain produced by structural motions: global and local. These can be caused by transient motions from blast vibrations, or quasi-static motions induced by settling and other longer-term causes. Global strains are produced throughout the structure by the gross motion of large structural members such as walls, floors and ceilings. Resulting global strains can be estimated using the equation for shear strain as shown in figure 2:

$$\varepsilon = \frac{1}{2} \frac{\Delta x}{y} = \frac{1}{2} \gamma \quad (2),$$

where

ε = axial strain

γ = shear strain

Δx = differential displacement

y = direction perpendicular to x

Hence, according to equation (2), strain is proportional to differential displacement.

Local strains arise from global strains and develop in relation to small-scale structural features such as corners and openings. At openings, local strain magnitudes can be greater than global strains due to quantifiable geometrically-induced strain concentrations. For instance, 90-degree square-cornered openings produce high stress concentrations which is why window and door openings are likely places to find cracks. Structure response to ground vibrations can also cause adjacent structural members to move differently, or out of phase, which also produces relative displacement and consequent strain.

The exact relationship between local strain, global strain and differential displacement depends on complex factors such as the shape of the deformation and the connection strength between adjacent structural members (Dowding, 1985). Also, cracking is more directly a result of local rather than global strains, effected by structural features that produce stress concentrations.

It can be said that increasing the differential displacement will increase local strains and thus the probability of creating cosmetic cracks near a stress concentrator or along an existing crack. Cracking generation or changes in existing cracks should correlate with the largest differential displacements (measured or calculated) at these locations.

Measurements of local and global strain, such as performed by Stagg et al. (1984) are a more direct approach to ascertaining cracking potential. Unfortunately, measuring strains directly requires expensive monitoring equipment and knowing the location of maximum strains for correct placement of gauges.

House Response

House response to ground vibration excitation is frequency dependent. This phenomena has been discussed by Siskind et al. (1980b), Dowding (1985), Crum and Siskind (1993), Crum and Pierce (1994), Pierce and Crum (1996) and a host of others. The observed frequency dependent response of structures is often described as the response of a damped single-degree-of-freedom system (SDF). The Duhamel SDF response model is used to simulate response to transient (finite duration) and complex excitation, like that produced by blast-induced ground motion. For this reason, the Duhamel model is often labeled a finite-duration SDF model (FDSDF). A form of the Duhamel integral to compute relative displacement from a measured velocity is:

$$\delta(t) = - \int_0^t \dot{u}(\tau) e^{-\beta 2\pi f_n(t-\tau)} \left\{ \cos[p_d(t-\tau)] - \frac{\beta}{\sqrt{1-\beta^2}} \sin[p_d(t-\tau)] \right\} d\tau \quad (3).$$

where:

$\delta(t)$ = relative displacement as a function of time.

$\dot{u}(\tau)$ = velocity as a function of the time shift variable τ .

β = fraction of critical damping (structural damping value).

f_n = natural frequency.

$p_d = 2\pi f_n \sqrt{1-\beta^2}$, the damped circular natural frequency.

(Note that equation 3 is a convolution integral and solvable by Fourier transform methods.)

The pseudo response-velocity (PRV) time function, $\dot{\delta}(t)$ (see Dowding, 1985), is obtained from equation (3) using the relation:

$$\dot{\delta}(t) = 2\pi f_n \delta(t) \quad (4).$$

Equation (3) will yield the same response for the closed-form SDF solution that assumes an infinitely long, continuous, sinusoidal, harmonic excitation, or IDSDF (infinite duration SDF), as described by Harris and Crede (1961). Crum and Siskind (1993) and Crum and Pierce (1995) incorporated the IDSDF model to describe observed structure response motions. Dowding (1996), however, argues that IDSDF is an inappropriate model for structure response to transient ground motion, and recommends the use of FDSDF. (Also see Langan, 1980, for a discussion on the application of FDSDF systems for modeling structure response.)

According to the general SDF theory, ground vibration at or near the structural natural frequency produces the largest potential response. Structure response to **natural frequency excitation** can be

several times greater than the amplitude of excitation. Amplification will decrease as excitation frequencies either increase or decrease away from the structural natural frequency. Figure 3 illustrates the frequency-dependent SDF response to infinite, continuous, sinusoidal, harmonic excitation.

Natural Frequency

The natural frequency of a structure is defined as the structure's lowest characteristic mode of response and can be measured during free vibration. Free vibration response occurs after all forcing vibration has ceased and, as depicted in figure 4, consists of simple, decaying, sinusoidal motion.

The structural natural frequency would ideally be determined from response to an impulse, which is an instantaneous signal of specified amplitude. In the frequency domain, an impulse function has uniform amplitude for all frequencies.

From the free vibration response time history, the structural natural frequency can be determined by the relation:

$$T = \frac{1}{f_n} \quad (5),$$

with T the period or time duration (in seconds) of one complete cycle of free vibration response and f_n is the natural frequency expressed in number of cycles per second, or Hz (hertz). The natural frequency range for typical one- to three-story wood frame homes is about 4 to 12 Hz (Siskind et al., 1980b).

Amplification

Amplification factors calculated from measured house-response for several Bureau of Mines studies including Siskind et al. (1980b), Crum and Siskind (1993) and Crum and Pierce (1995) are shown in figure 5. Structural amplification is most correctly computed as the maximum or peak high corner structure response amplitude divided by the amplitude of the driving ground vibration. The "driving" ground vibration is defined as the portion of the ground vibration that, upon interpreting the time history, appeared to causing maximum structure response. The relationship between maximum ground vibration, driving ground vibration and maximum structure response is illustrated in figure 6. The amplification factors shown in figure 5 were calculated relative to peak structure response, which usually occurs in the horizontal direction of motion.

Homes can exhibit a high corner response amplitude as high as 2- to 5-times the amplitude of the driving ground vibration excitation. High corner amplification is usually dominant in the horizontal directions of motion. Although the highest amplifications are found within the natural frequency range for homes of 4 to 12 Hz, the extent of amplification values for any particular frequency varies significantly.

According to Dowding (1996, personal communication), higher structural amplification increases the amount of differential motion, and thus strain, as described in equation (2). Therefore, house response to ground vibration frequencies at or near the structural natural frequency, where the highest structural amplification is expected, is more likely to produce greater strain in structures compared to higher or lower ground vibration frequencies with similar amplitudes.

Damping

According to SDF theory, the maximum amount of potential structural amplification is dependent on vibration-damping characteristics of the structure. For a given excitation amplitude with a frequency equal to the structural natural frequency, a structure with lower damping will have a greater maximum potential amplification compared to a structure with higher damping.

Structural amplification decreases as excitation frequencies either increase or decrease away from the natural frequency. Based on SDF theory, structural amplification will tend to unity as excitation frequencies decrease below the structural natural frequency and towards zero as excitation frequencies increase above natural frequency, becoming equivalent at either end of the spectrum regardless of damping characteristics (see Crum and Pierce, 1995).

Damping can be calculated from the structure's free vibration response. The equation for computing damping given by Dowding (1985) is:

$$\beta = \frac{1}{2\pi} \left(- \ln \frac{\dot{u}_{n+1}}{\dot{u}_n} \right) \quad (6),$$

where β is the damping expressed as a percent of critical, and \dot{u}_n and \dot{u}_{n+1} are the crest (or trough) amplitudes of successive cycles of free vibration response (see figure 4).

Typical damping values measured for homes range from about 1 to 10 pct of critical (see RI 8507, figure 32). Dowding (1985) lists an average damping value of 5 pct for residential structures. Because of differences in damping, taller buildings generally have lower damping characteristics than shorter structures and will generally produce higher amplifications. Similarly, structure response amplitude will ordinarily increase with increasing height above the ground.

Quasi-Free Vibration

Although structural natural frequency and damping are ideally calculated from free vibration response, houses rarely exhibit *true* free vibration. Careful examination of ground vibration and corresponding structure response recordings show that almost all structural motion is associated with at least some ground vibration excitation. Therefore, in relation to house response, *quasi*-free vibration would more accurately describe what has in the past been termed "free" vibration.

Analysis used in this report found that consistent measurements of natural frequencies could be made from quasi-free vibration response. However, free response equations for damping, such as equation (6), may not be practical for computing the damping of homes. Any latent excitation would influence computed damping values. Dowding (1985) recognizes this problem and suggests the use of transfer function methods, which were not evaluated in this investigation.

GROUND VIBRATION AND STRUCTURE RESPONSE MEASUREMENTS

To find suitable monitoring sites for this study, Bureau of Mines researchers contacted 21 different surface blasting operations in 10 states. Some of these sites included recommendations from citizens, regulators and mining personnel, and involved 20 coal mines and one land development project. The initial criteria for final site selection included: 1) One or more homes in structurally sound condition that were available for monitoring; 2) ground vibrations at the home(s) with dominant frequencies below the structural natural frequency and amplitudes greater than 0.5 in/s (the minimum amplitude threshold for cracking established by RI 8507 for ground vibration frequencies above 4 Hz); 3) necessary access to the home(s) for monitoring and 4) cooperation of the mining company to coordinate logistics for monitoring.

After initial telephone interviews with mine officials, researchers made follow-up visits to the most promising sites for inspection and preliminary monitoring. In all, only three of the initial 21 sites had houses, either occupied or abandoned, that were being impacted by low frequency ground vibrations and peak³ ground vibration velocities above 0.5 in/s. Hence the site selection process led to an early conclusion that the occurrence of low frequency ground vibrations with the potential to cause cracking or worse forms of damage in homes is not common and could even be considered rare.

Because of the difficulty in locating appropriate monitoring sites, criteria 2 was expanded to include dominant ground vibration frequencies that were equal to, or above the structural natural frequency. By modifying the selection criteria, it was hoped that enough relevant information could be obtained on structure response and vibrations-induced cracking to enhance the current level of understanding of blast-induced ground vibrations and their effects on structures.

Test Homes

In all, ten homes were studied over the course of the investigation. Table 1 describes the test homes and their locations. Photographs of some of the test homes are included as figures 7 through 13. Of the nine wood frame homes studied, seven were located near three different Indiana surface coal mines and two were adjacent to a surface coal mine Pennsylvania. The other home was located at a Florida land-development site, the Arvida "Plan B" house (not shown),

³ Peak ground vibration velocity, often referred to as "peak particle velocity", is the highest absolute-value measured ground vibration velocity for an individual event, relative to all three components of motion. Maximum ground vibration velocity, a term also used in this report, refers to the highest ground vibration velocity for a single component of motion. e.g., there is only one peak ground vibration velocity per event but three maximum velocities.

which was built according to hurricane resistant standards with cement-block walls and poured concrete caps. The Arvida house was included in the study because it represented a different type of construction respective to the more common wood-frame homes that have been examined by the Bureau of Mines in the past.

All of the homes except the McConnell home were, at some point in the study, monitored for ground vibrations and structure response. Table 2 lists the names of the monitored homes and relevant information such as the number of blasts monitored, information on crack inspection procedures and a summary of indexed blast vibration levels.

Monitoring

The majority of ground vibrations and structural response recordings were made using Mini-Seis⁴ blasting seismographs, shown in figure 14. The sensor package, or "geophone", contained the three orthogonal-aligned accelerometers. For ground vibrations monitoring, the geophone was installed by shallow burial method, as illustrated in figure 15. Motion is measured initially as acceleration and converted to velocity by an analog circuit before digital recording by the seismograph. According to the manufacturer's specifications, this system enabled the recording of vibrations from 2 to 200 Hz within ± 3 dB. Because the geophones contained accelerometer transducers, they could be installed in any orientation. This was convenient for structural monitoring because the geophones could be vertically attached to a wall without the need for angle-brackets.

For structure response monitoring, the geophones were attached to walls or joists using 3-in x 3-in aluminum plates that had a bolt head fixed at the center (shown in figure 16). The plate was securely screwed into the corner wall stud in a vertical position with four 2-1/2-inch long masonry screws. The bottom of the transducer contained a recessed opening with a side set-screw to secure the transducer to the plate. Because the entire geophone package weighed only about one pound, it did not add appreciable mass to the structure and therefore did not affect the response. Figure 17 shows a Mini-Seis transducer set-up for high corner response monitoring inside the Shack.

Recording of time-synchronized ground vibration and structure response was accomplished using the standard "daisy-chain" feature of the seismograph. This allowed a selected master unit (usually the one installed to detect ground motion) to simultaneously trigger several other "slave" units chained together in series. The manufacturer's estimate of the time delay in triggering a slave unit from the master is 1 millisecond (1/1000 of a second).

Seven of the test homes were instrumented to record ground vibrations and structure response using the Mini-Seis seismographs: these houses were the Shack, Manor, Hole, Smith, Lhemkuhler, Pritcher, and Arvida. Monitoring at the Hoover and Jordan homes (described in Crum and Siskind, 1993, and Crum and Pierce, 1994, respectively) was undertaken before Bureau

⁴ The Mini-Seis seismographs were manufactured by Larcor (Quinlan, Texas) and distributed by White Seismology (Joplin, Missouri). The Mini-Seis seismographs used in this study were obtained from Vibronics of Evansville, Indiana.

acquisition of the Mini-Seis units, and utilized an accelerometer-based FM tape-recording system that also provided time-synchronized ground vibration and structure response recordings. Only ground vibrations were recorded at the McConnell house, but pre- and post-blast crack inspections were regularly performed during the course of study at this home (see Crum and Pierce, 1994).

Figure 18 contains histograms of maximum ground vibration amplitudes measured at the Shack. The Shack was the principal low frequency site because of the high amplitude, low frequency ground vibrations monitored there. However, as indicated in figure 18, the occurrence of both high amplitude *and* low frequency ground vibrations from the same blast was not common (for the Shack, low frequency would be below the natural frequency of about 5.5 Hz).

Observations Based on Full-Waveform Recordings

Representative ground vibration and structure response recordings were selected to further illustrate the principle of frequency-dependent structural response. Figures 19 and 20 show complete sets of ground vibration and structure response recordings obtained at the Jordan house for two different blasts. Corresponding structure response at three different locations in the house are shown along with the ground vibrations. Both sets of records indicate low frequency ground vibration at about 2.5 Hz, below the calculated structural natural frequency of 6 Hz. The ground vibration in figure 20 shows very dominant 2.5 Hz horizontal motion at relative maximum amplitudes. Ground vibration and structure response recordings from these events will be discussed in more detail later on.

Response to Excitation at the Structural Natural Frequency

Figure 21 shows the ground vibration and structure response measured at the Shack. The corresponding Fourier frequency spectra, obtained using a Fast Fourier Transform (FFT) algorithm⁵, is also shown. This example is typical of several monitored events at the site.

The ground vibration is predominantly 6 Hz which is almost identical to the structural natural frequency - a classic example of response to excitation at the structural natural frequency. Note the similarity between the ground vibration and structure response frequency spectra, including the 6 Hz peak on both.

The maximum structure response of about 3 in/s, occurring at 1.6 seconds, originates from one or two continuous cycles of approximately 1 in/s ground vibration excitation near the structural natural frequency. The resulting structural amplification factor is about 3-times, similar to amplification expected from excitation at the structural natural frequency as discussed above.

⁵ A fast Fourier transform (FFT) algorithm was used to compute the all the frequency spectra analysis discussed in this report.

Response to High Frequency Excitation

More complex ground vibration and structure response are shown in figure 22 - measurements made at the Jordan house. Figure 22a corresponds to the N-S component of the ground and high-corner response shown in figure 19. Figure 22b similarly corresponds to the N-S component in figure 20. The inset in figures 22a and 22b shows the early portion of the ground vibration and structure response time history at an expanded scale. This can be considered the high frequency portion of the ground vibration, most directly influenced by the explosive detonation and the individual delay sequencing used in the blast. Predominant ground vibration frequencies within this portion are near 30 Hz, which is about 5-times greater than the 6 Hz natural frequency of the structure. There is a very small amount of relative structure response to this high frequency excitation. Most of the structure response in this part of the time history is associated with the lower frequency component coupled to the higher frequency excitation. At a time of about 1.5 seconds in figure 22a, the frequency of the ground vibration approaches that of the structural natural frequency, creating the type of natural frequency response that was also seen in figure 21. The change in ground vibration frequency from higher to lower frequencies is largely due to the effects of the ground on vibration energy. High frequency ground vibration is also observed in the early part of figure 22b (corresponding to figure 18) with correspondingly similar structural response as the high frequency portion in figure 22a.

Response to Low Frequency Excitation

The low frequency portion of the ground vibration in figure 22b becomes dominant at about 0.75 seconds. The predominant frequency is about 2.5 Hz, approximately half the structural natural frequency. Except for some structural amplification at the peaks and troughs, house response closely resembles the ground vibration. This type of response is consistent with discussions in all elementary structural dynamics texts (Dowding, 1996, personal communication) and illustrates an example of field observation conforming to theory. Maximum structure response in figure 22b occurs at about 0.9 s with an amplification factor of approximately 2-times. An amplification of about 1-time is theoretically expected from excitation frequencies at $\frac{1}{2}$ the structural natural frequency. The difference between measured and theoretical structural amplification from low frequency excitation gives an example of how real-world response measurements may differ from theoretical expectations. However, the 2-times amplification is similar to, or less than values expected for structure response from natural frequency excitation.

Note that the significant amount 6 Hz response in the structure response Fourier spectra of figure 22b, even though there is almost no 6 Hz energy in the ground vibration. This serves to illustrate the efficiency at which structures respond to excitation energy at the structural natural frequency. However, because of the overwhelming amount of low frequency energy, the amount of 6 Hz response is significantly less than that pertaining to the 3 Hz, low frequency excitation.

Effects of Ground Vibration Duration on Structure Response

According to SDF theory, structural amplification from excitation at the structural natural frequency is expected to increase with the number of continuous, harmonic, sinusoidal excitation

pulses up to the maximum potential value which is dependent on structural damping. A structure with a higher damping will require fewer continuous, harmonic, sinusoidal excitation pulses at the natural frequency in order to achieve maximum response. This effect is illustrated in figure 23 showing results obtained using equations (3) and (4) and a varying number of continuous, harmonic, sinusoidal excitation pulses at the system natural frequency.

The actual influence of ground vibration duration on maximum structure response cannot be quantified by measurements or observations made in this study nor any other investigation that the author is aware of. Blast-induced ground vibration does not ordinarily exhibit continuous, harmonic, sinusoidal motion. At best, no more than two or three cycles of ground vibration are found that even resemble continuous, harmonic, sinusoidal motion, as shown previously in figure 21, the ground vibration and structure response recordings at the Shack. Therefore it is often argued that the potential exists for structural amplification higher than the worse-case 3- to 5-times typically found for homes, if an anomalous, long duration, harmonic, sinusoidal ground vibration were produced with a dominant frequency that matched structural natural frequency. This, it could be debated, would produce extreme structural amplification and induce cracking even if excitation amplitudes are below expected safe-levels. Low amplitude portions of the ground vibration that occur late in the time history at distances greater than two or three miles sometimes produce amplifications of 5- to 10-times relative to that portion of the vibration (e.g., not relative to the maximum structure response). The actual response amplitude from this low amplitude excitation is, however, much less than the measured maximum response amplitude.

Natural Frequencies of the Test Homes

Structural natural frequencies were determined for nine of the ten homes studied during the overall investigation and are listed in table 1 (the McConnell home was not instrumented for structure response and therefore the natural frequency could not be determined).

Natural frequencies determined from the structure response time histories used the period inversion approach exemplified by equation (5). The period of the natural frequency was measured from the quasi-free response portion of the structure response time history. Structural natural frequencies calculated from period inversion were compared to those obtained from the Fourier frequency spectra computed for the response time histories recorded by the seismographs. The Fourier frequency spectra usually contained a single dominant frequency or narrow range of dominant frequencies that matched the natural frequencies obtained from the quasi-free response portion of the response time history. Ultimately, Fourier analysis was preferred for determining natural frequency as opposed to period inversion because the Fourier approach was accurate, less ambiguous and allowed for faster analysis.

High-corner horizontal structure response motions were usually dominated by a narrow range of "characteristic" frequencies that deviated by only about one or two Hz from a mean value. The range of these characteristic frequencies remained consistent for a specific home even though ground vibration frequencies were more variable and spanned a much broader range. This consistency demonstrated that the dominant response frequencies were reflecting the natural

frequency characteristics of the house. The average of the home's characteristic frequency range was interpreted as the natural frequency.

Care was taken not to misinterpret response from low frequency excitation, as exhibited in figure 22b, as a characteristic or natural frequency response. This was done by cross-checking frequencies calculated from the high corner response time histories with the corresponding Fourier frequency spectra.

High corner vertical-component structure response frequencies were usually similar to the corresponding ground vibration frequencies in the vertical direction and not considered representative of any distinct global structural response property. Therefore, only the horizontal high corner structure response was employed to determine natural frequency.

Although house types varied considerably, the eight wood-frame homes had remarkably similar natural frequencies between about 5 and 7 Hz. For example, the two most different house types - the Shack, a small, single-story bungalow with wood siding and the Jordan house, a large, three story farmhouse with brick siding and a slate roof - possessed similar natural frequencies of about 5 to 6 Hz.

Based on the common assumption that house response is similar to that of a single degree of freedom system, the structural natural frequency is related to the structural properties by:

$$\omega_n = \sqrt{\frac{k}{m}} \quad (6)$$

where

$$\begin{aligned} \omega_n &= \text{circular natural frequency} = 2\pi f_n \\ k &= \text{stiffness} \\ m &= \text{mass} \end{aligned}$$

The larger farmhouse would be expected to have a distinctly lower natural frequency than the smaller bungalow because of their apparent differences in size and construction materials. However, observations made in this study generally indicate that structurally-sound wood-frame homes should behave similarly when excited by blast-induced ground vibrations. It is possible, though, that the brick exterior of the Jordan house increased the structural stiffness, compensating for its larger size.

The block and concrete home at the Florida land-development site was more highly damped and much stiffer than the other wood-frame homes. Only at the high corner of the tall, 11-foot high wall of the "great room" could natural frequency-type response motions be measured. (The ceiling of the "great room" was higher than any other room in the house and also much higher than any of the ceilings in the wood-frame test homes, all of which were normally between 7 and

8 feet tall.) The natural frequency measured at the Florida home was found to be 11 Hz, significantly higher than the wood-frame houses.

Structural Amplification of Ground Vibration

Amplification factors were computed for five of the test homes: Shack, Smith, Lhemkuhler, Jordan and Arvida. (Preliminary results from the Shack, Smith, Lhemkuhler and Jordan houses were presented in Crum and Pierce, 1995). These homes were chosen because of their association with different blasting operations and are considered representative of a wide variety of house types. The frequency of the maximum ground vibration was computed from the reciprocal of the period, P , of the portion of the ground vibration containing the highest absolute-value velocity:

$$f = \frac{1}{P} \quad (7),$$

with f being the frequency in Hz or cycles per second and P is the period (in seconds) for one complete vibration cycle. The relation is similar to equation (5) except that P is not necessarily a period of free vibration. Using equation (7) an absolute amplitude can be assigned to the frequency whereas the Fourier frequency spectra produces only relative amplitudes for the individual frequency components.

The houses at the Amax Minnehaha site; Shack, Manor, and Pritcher, exhibited similar types of structure response. The Shack was chosen to represent the Minnehaha site because it was the closest structure to the blasting that was in acceptable condition. The Hole was actually closer to the blasting than the Shack, but the Hole was in extremely poor repair and severely damaged from non blasting causes, such as looting and close approaches by heavy equipment. Although some studies may be interested in the response of such disheveled structures, the purpose of this investigation was to characterize more typical types of homes and thus the Hole was dropped from the study after a few measurements were made.

Ground vibration and structure response measurements at the Hoover house were presented in Crum and Siskind (1993). The Hoover house was the first home monitored for the low frequency study as part of a preliminary investigation prior to the larger endeavor. The ground vibration and structure response amplitudes at the Hoover house were much lower than for the other sites (below 0.05 in/s) and the quality of the data was poor compared to those obtained in subsequent monitoring. The measurements made at the Hoover home are therefore not included in this report.

Preliminary monitoring at the Shack, Lhemkuhler, Jordan and Arvida houses involved measuring structural response at several different high and low corners at each structure. Analysis indicated that the largest structural amplification of ground vibration excitation occurred at the "leading edge" of the structure, or the side of the house situated closest to the blast. Amplification at other corners from the same vibration did not exceed that found at the leading edge, being either equal to or less than leading edge amplification. The Arvida house was an exception because the only

distinct structurally-induced responses came from the high corner of the great room which was not always closest to the blast.

A few midwall response measurements were also made in conjunction with the corner monitoring. Midwall dimensions were generally smaller than ceiling heights and usually contained windows or doorways. This created relatively stiff midwalls, and resulted in maximum midwall response amplitudes that were similar to or less than the corresponding high corner response.

Three of the test homes - Shack, Lhemkuhler and Smith, all located near different surface coal mines in Indiana - were subjected to relatively high amplitude ground vibrations from over 0.5 in/s (to 6.0 in/s at the Shack) with a broad range of dominant frequencies below, at, and above the structural natural frequency. The Jordan home and the Arvida Plan B house experienced blast vibration frequencies at about $\frac{1}{2}$ the structural natural frequency. These were the lowest frequency ratios found at any of the five test homes. Peak ground vibration amplitudes at these houses were below 0.5 in/s. At the Jordan house, peak ground vibration amplitudes averaged 0.18 in/s with 0.27 in/s being the highest. Peak ground vibration amplitudes measured at the Arvida home averaged 0.21 in/s with 0.44 in/s being the highest.

Data Reduction

The structure response data was systematically reduced in number to simplify analysis and decrease the amount of redundant information that would be displayed in the graphs. Upon careful examination of all the ground vibration and structure response information, the recordings from 10 blasts at the three wood-frame homes and five blasts at the Florida home were selected as representative examples. Ground vibration and structure response from two of the four blasts monitored at the Jordan house were also used. Of the other two blasts at this site, one was not recorded due to operator error and instrumentation problems precluded the analysis of the other event.

The set of 37 selected events constitutes a representative range of amplitudes and frequencies for both ground vibration and structure response that were encountered during the study. Driving ground vibration amplitudes and frequencies for the 37 representative events are shown in figure 24 and are listed in Appendix A along with values from structure response measurements. Again, the driving ground vibration is the portion of the vibration time history that appeared to produce maximum structure response (refer to figure 6). This type of analysis is consistent with that used by Bureau of Mines researchers in developing the safe-level recommendations published in RI 8507. The representative data span a frequency range of about 2.5 to 80 Hz with amplitudes between 0.04 to 6.0 in/s. Excitation frequencies for ground vibrations exceeding 0.5 in/s fall between 5 and 30 Hz.

The directions of motion identified in the figures 24 and 25 (following) and Appendix A are a convention used throughout this report that relate the components of recorded motion to the configuration of the structure rather than to the orientation of the blast. The radial direction is defined as being parallel to the major (longest) roof line (or perpendicular to the alignment of the roof trusses), the transverse direction is perpendicular to the major roof line (or parallel to the

alignment of the roof trusses), and the vertical direction is normal (perpendicular) to the floors and ceilings.

Results

Figure 25 is a plot of amplification factor versus frequency ratio for the five test homes. Amplification factor was computed as maximum structure response velocity divided by the velocity of the driving ground vibration, calculations that are again consistent with those used for the RI 8507 study. The frequency ratio is the frequency of the driving ground vibration divided by the structural natural frequency determined from horizontal component motion (see table 1). Note the similarity between the amplification-frequency relationship for the four test homes shown in figure 25 (horizontal direction) with that displayed in figure 5 (for figure 5, assume a structural natural frequency range of 4 to 12 Hz). Although there is considerable scatter in the data, there is a definite observable trend towards higher horizontal-component amplification from ground vibration frequencies corresponding to the structural natural frequency.

The information presented in figure 25 addresses the concern expressed earlier about the effects of low frequency ground vibrations. Measured low frequency ground vibrations below 0.9-times the structural natural frequency produced similar or lower amplification compared to higher frequency ground vibrations. In addition, maximum amplification from low frequency ground vibrations were less than worse-case of 3- to 5-times amplification associated with ground vibration frequencies at or near the structural natural frequency. Following the assumption that higher amplification creates higher strain and cracking probability, then low frequency ground vibrations should not warrant special concern for induced structural cracking compared to higher frequency ground vibrations - a conclusion expressed previously by Crum and Pierce (1994).

The vertical-component data in Figure 25 indicates that significant amplification can also occur in the vertical direction, with magnitudes comparable to the largest horizontal amplifications. Vertical component structural motions have not typically been identified with generating 2- to 4-times amplification, as is seen from the data. Vertical driving ground vibration amplitudes, plotted in figure 24, are almost all above 0.1 in/s and therefore the higher vertical amplifications are not likely the result of a very small ground vibration amplitude being divided into the structure response amplitude.

Vertical component amplifications in figure 25 are shown as a function of vertical driving ground vibration frequency divided by the structural natural frequency that was determined from horizontal response motions. (Recall that vertical component response frequencies are similar to ground vibration frequencies and do not exhibit distinct motion characteristics of the structure such as natural frequency.) This was done so that the frequency axis for the horizontal and vertical component data in figure 25 would be similar: For example, at a particular structure, the horizontal component driving ground vibration frequency at 2-times the natural structural frequency would be the same as the vertical component driving ground vibration frequency at 2-times the natural frequency.

It may be inappropriate, therefore, to analyze the vertical component amplification data in terms of a SDF system as was done with the horizontal component data. Regardless, there is a noticeable relationship between higher vertical amplification and higher vertical ground vibration frequencies at most of the test homes. The Jordan house experienced only consistently high vertical driving ground vibration frequencies.

The significant vertical amplification from high frequency excitation may be reason for concern regarding structural cracking because of the possibility of inducing vertical tensional strains or a decoupling of the superstructure from the foundation. High amplitude, high frequency ground vibrations are more commonly produced from construction blasting than from mining or quarrying (see Siskind et al., 1980b).

Response Velocity vs. Ground Vibration Velocity

A strong statistical association was identified between maximum ground vibration velocity and high corner structure response velocity, as shown in figure 26. The regression line shown in the figure has the form:

$$\text{Log}(y) = m \cdot \text{Log}(x) + b \quad (9);$$

where y is the vertical axis, x is the horizontal axis, m is the slope of the regression line, and b = log(y) at log(x) = 1. The regression line represents the statistical mean of the data.

The regression line in the figure 26 is plotted as

$$y = x^m \cdot 10^b \quad (10),$$

achieved by raising both sides of equation (9) to the power of 10.

The standard deviation, σ , was also determined from the log-transformed x and y values and is a measure of the variability of the y-variable with respect to the x-variable (the standard deviation is defined as the square of the variance). Although not shown in the figure, the plus-minus standard deviation envelope can be obtained by:

$$y_{\pm} = x^m \cdot 10^{(b \pm \sigma)} = y \cdot 10^{\pm \sigma} \quad (11).$$

The r^2 coefficient shown in figure 26 is the correlation coefficient squared, thought to be a better measure of x-y interdependence than simple correlation. The correlation coefficient has a range of values between -1 and +1, and therefore the r^2 term has a range of values between 0 and +1. Although better used as a relative indicator of statistical significance, an r^2 of 50 pct or higher (i.e., $r^2 \geq 0.5$) usually indicates significant dependence between the x and y variables; the higher the r^2 value the higher the significance. A smaller value of r^2 for similar data sets will correspond to a higher amount of standard deviation.

In figure 26, the r^2 value of about 61 pct for the horizontal direction indicates a good statistical association between high corner and maximum ground vibration velocities. The r^2 of 93 pct found for the vertical direction shows a stronger statistical association with a slope near unity (on a log-log scale).

Figure 27 shows the relationship between driving ground vibration and maximum ground vibration. The statistics used coincide with those used for the previous figure 26. While not necessarily the same as the ground vibration phase, the amplitudes of the driving ground vibrations are on average very similar to maximum ground vibration amplitudes.

OBSERVATIONS OF BLAST-INDUCED CRACKING

Four of the test homes - the Jordan and McConnell houses in Pennsylvania, and the Shack and Lhemkuhler house in Indiana - were studied to ascertain if blast vibration-related cracking was produced. The Florida home was new and no interior or structural cracks could be found other than very minute cracks assumed to be associated with paint and plaster drying, nor were any cracks observed to have occurred during monitoring at the structure. The other homes were unsuitable for crack inspections because of inaccessibility or that the walls were covered from view with wall paper or paneling that could not be adequately removed (this was the general situation at the Manor, Hole and Smith).

The Hoover home was about 5 miles from the blasting and received ground vibration amplitudes less than 0.05 in/s. Because of the extremely low amplitudes, blast vibrations-induced cracking was extremely unlikely and a cracking study at this home was not undertaken. (A previous Bureau of Mines blast vibrations study in the vicinity of the Hoover house, Siskind et al., 1993, found no blast-vibration related cracking from similar amplitude ground vibrations.)

Procedure

The visual crack investigation undertaken in this study was very similar to those used in previous studies described by Siskind et al. (1980b; 1993). Observations for interior cracking were made to identify the lowest ground vibration levels necessary to cause cracking or crack changes. Interior finishing materials, such as wallboard and plaster, have a much lower resistance to vibrations-induced cracking than concrete or masonry typically used for foundation construction and exterior finishing.

The test homes were initially inspected to identify locations inside the home that contained cracks. Strain concentrating areas were examined and consisted of inside corners including doorways, window openings, inside walls and ceilings. Masonry joints are also susceptible to cracking, but were not studied because of the higher levels of motion necessary to cause cracking and because of the difficulty to identify cosmetic cracking in mortar or at the brick-mortar interface.

Crack growth - extensions in crack length - are usual forms of vibration-related cracking. To study crack growth, cracks with a definite end need to be identified. These cracks were always

threshold-type and were usually less than a few tenths of a millimeter wide. Preexisting crack ends were marked and examined for change. Larger cracks, about one to three millimeters wide, would usually span from corner to corner without an observable mid-span terminus. These types of cracks were used to study crack-width changes at a fixed location on the existing crack. Corner areas without observable cracks were also examined for the formation of new cracks.

Several locations inside each of the homes were used to monitor crack change (see table 2). Inspections for vibration-induced cracking were made by careful visual pre- and post-blast observations performed within about five minutes before and after each blast, respectively. Inspections were made with 7-power optical magnifiers with 0.1 mm optical scales. Inspection areas were illuminated with flashlights or, more ideally, with automotive trouble lights with 100 watt bulbs. Figures 28 and 29 depict a researcher performing crack inspections with the 7-power optical magnifier.

Results of the Crack Investigation

A total of over 350 individual pre- and post-blast inspections for interior cracking were made at the four homes from 46 monitored blasts. About 70 pct of the these blasts (all in Indiana) produced peak ground vibration velocities of 0.5 in/s or greater with the highest peak ground vibration amplitude recorded at 6.0 in/s. However, only two occurrences of blast vibrations-related cracking were observed: one each at the Lhemkuhler house and the Shack. Both of these instances of cracking can be classified as cosmetic, and would be very difficult to detect without the rigorous inspection techniques that were applied.

The peak ground vibration amplitudes and frequencies of the crack-causing and non-crack-causing events for the 46 monitored blasts are shown in figure 30. Driving ground vibration amplitudes and related frequencies corresponding to the two observations of cracking plotted in figure 31 along with the cracking observations and safe-level criteria recommendations published in RI 8507. (The use of driving ground vibration values, rather than peak values, is consistent with the analysis methods incorporated in the RI 8507 study.)

The instance of observed blast-induced cracking at the Lhemkuhler house involved the generation of a new hairline crack in plaster that was less than 0.05 millimeter wide. The driving ground vibration corresponding to peak structure response had an amplitude of 0.53 in/s at 6.4 Hz. Peak structure response was 1.26 in/s (also at 6.4 Hz) resulting in an amplification factor of 2.4-times. The peak ground vibration recorded for this blast monitored the Lhemkuhler house was 1.44 in/s with a frequency of 39.3 Hz⁶. The other occurrence blast vibrations-induced cracking was noted at the Shack, observed as a crack width change of a about 0.05 millimeter. The driving ground

⁶ Peak ground vibration and structure response amplitudes and frequencies for this event at the Lhemkuhler house were taken from the readings automatically calculated by the seismograph in order to be consistent with the time histories presented in Appendix B. The values differ slightly than those reported by Crum and Pierce (1995) which used alternative manual measurements of ground vibration and structure response amplitudes obtained with the aid of analysis software. The digital ground vibration recording of the crack-producing event at the Lhemkuhler house was inadvertently destroyed and Crum and Pierce (1995) used a digitized copy of the paper record which may have altered the amplitude and frequency characteristics compared to the original seismograph recording.

vibration amplitude was 1.28 in/s at 5.6 Hz and the corresponding peak structure response was measured at 2.24 in/s (at 5 Hz), giving an amplification of 1.75-times. The driving ground vibration in this case was also the peak. As shown in figure 31, the ground vibration levels from both of these events exceeded the RI 8507 recommendations, sustaining the validity of the criteria. No other crack changes were observed at the homes from these blasts. The peak and driving ground vibration amplitudes of with these events were exceeded at the structures without an additional observed occurrence of cracking.

Appendix B contains the ground vibration and structure response recordings for the events recorded at the Shack and Lhemkuhler house identified with vibrations-induced cracking (Lhemkuhler 4/11/94 @1555 and Shack 10/12/93 @ 1236, respectively) along with other selected ground vibration and structure response recordings made during the study.

Airblast

Airblast was also monitored at the test homes along with ground vibrations and structure response. The larger airblast amplitudes were obtained at the Shack, Lhemkuhler and Smith houses with peak levels primarily between 115 and 125 dB, although there were several events at about 135 dB (a difference of 20 dB is equivalent to an order-of-magnitude change). The airblast amplitudes were recorded on a 2 Hz high-pass system. Siskind et al. (1980a) recommends 133 dB for 2 Hz high-pass monitoring systems as a maximum safe airblast level (equivalent to 134 dB on a 0.1 Hz high-pass system). This guideline is aimed at preventing window pane breakage, and threshold-level plaster cracking is not likely to occur until higher peak amplitudes are achieved. In general, airblast from surface mine blasting is not likely to cause cracking of plaster, drywall or masonry.

No window pane breakage was observed during the study and no evidence of airblast-related cracking was found. For the two observed occurrences of blast-related cracking at the Shack and Lhemkuhler house discussed in the previous section, the peak airblast levels were 114 dB and 127 dB (2 Hz system), and did not exceed the 133 dB threshold.

CONCLUSIONS

- 1) The occurrence of low frequency (i.e., below the structural natural frequency) blast-induced ground vibrations with the potential to cause cracking in homes is rare and not likely to be found in association with surface coal mining.
- 2) SDF theory indicates that structural amplifications could be produced that are much higher than the maximum 2- to 5-times amplification ordinarily found if ground vibrations contained many continuous cycles of harmonic, sinusoidal motion with a frequency that matches the structure's natural frequency. However, blasting does not produce this type of ideal ground motion at amplitudes that would cause reason for concern. Therefore, it is unlikely that ground vibrations from blasting will illicit the maximum structural responses predicted by SDF theory at levels that could cause structural cracking or damage.
- 3) Structural natural frequencies were determined from ground vibration-induced structure response using Fourier frequency spectra. (Time-domain period inversion methods were used to establish the accuracy of the Fourier approach.) Despite the sampling of a wide variety of house types, measured structural natural frequencies for wood-frame houses were surprisingly consistent and ranged between 5 and 7 Hz. A newer concrete block house had a **calculated natural** frequency of 11 Hz.
- 4) Worse-case structural amplifications of 3- to 5-times resulted from ground vibration frequencies between 0.9- and 2-times the structural natural frequency, in agreement with previous reports. Calculations of structural amplification indicate that low frequencies do not pose any particular or unusual threat of cracking to houses. Structural dynamics theory indicates that larger structural amplification corresponds to an increased potential for cracking. Structural amplifications from low frequency ground vibrations were similar to or lower than amplifications produced from higher frequency ground vibrations. Worse-case amplifications were associated with ground vibration frequencies near the structural natural frequency and therefore correspond to the highest theoretical potential for cracking.
- 5) A detailed study of pre- and post-blast crack observations found that the occurrence of even threshold and minor cosmetic cracking in homes from blast vibrations is extremely rare. Inspections for interior cosmetic cracking were made in relation to blasts that produced maximum ground vibration amplitudes from less than 0.5 in/s to 6.0 in/s. Of the two incidences of cosmetic cracking that were found, ground vibrations from one blast caused a small change in an existing minor cosmetic crack and another event created a new threshold-level cosmetic crack. For both of these events, the driving ground vibration amplitude associated with peak structure response exceeded the Bureau of Mines RI 8507 safe-level recommendations for avoiding structural cracking in homes.
- 6) Although peak airblast levels measured at some of the test homes were as high as 135 dB (2-Hz high-pass), there were no indications that any airblast caused cosmetic interior cracking or window breakage.

ACKNOWLEDGMENTS

Funding for this project was principally provided by the Bureau of Mines before its closure in February, 1996. The Office of Surface Mining, under the guidance of Ken Eltschlager with support from Roger Calhoun, supplied additional funding for completion of this manuscript. Dr. Charles Dowding furnished an exhaustive review of the draft report and provided many constructive comments and suggestion to improve the contents. Mr. Eltschlager, Dennis Clark and Mike Rosenthal, Dr. David Siskind, Mark Stagg and Steve Weinzapfel also provided detailed technical and editorial reviews. Your efforts are greatly appreciated.

I would also like to thank the many other individuals, companies and government agencies who helped make this study possible: John Brown, Dr. Alan Perry, Steve Cummings, Larry Cornelius (Larcor), Randy Wheeler (White Seismology), John Wiegand (Vibronics), Brent Webber (Amax), Mike Sponslor and Alan Johnson (Indiana Dept. of Natural Resources), Ray Judy (Phoenix Natural Resources), C. William (Bill) Brewer (Arvida), Jeff Straw (Geosonics), Mike Cave (C&K Coal Co.) and Mike Getto (Pennsylvania Dept. of Environmental Protection); Amax Coal Company and Phoenix Natural Resources; Mrs. Hoover, Matt Smith, Paul Jordan and Yvonne McConnell; and to those persons or associations contributing to this effort that we may have inadvertently omitted.

REFERENCES

- Crendwelge, O. E., 1987, *Method for Determining Frequency Components of Blast Induced Ground Vibrations*, Shell Development Company.
- Crum, S. V., D. E. Siskind, 1993, *Response of Structures to Low Frequency Ground Vibrations: A Preliminary Study*, Proc. of the 9th Annual Research Symp. on Explosives and Blasting Technique, International Society of Explosives Engineers, San Diego, CA, pp. 149-161.
- Crum S. V. and W. E. Pierce, 1995, *House Response to Low Frequency Ground Vibrations From Surface Mine Blasting: A Technical Update*, Proc. of the 11th Ann. Research Symp. on Explosives and Blasting Technique, Intl. Soc. of Explosives Engineers, Nashville, TN.
- Dowding, C. H., 1985, *Blast Vibration Monitoring and Control*, Prentice-Hall, Inc., Englewood Cliffs, NJ, 297 pp.
- Dowding, C. H., 1996, *Construction Vibrations*, Prentice-Hall, Inc., Englewood Cliffs, NJ.
- Harris, C. M. and C. E. Crede, 1961, *Shock and Vibration Handbook, Vol. 1*, McGraw Hill, New York.
- Langan, R. T., 1980, *The Use of the Single-Degree-of-Freedom System as a Dynamic Model for Low-Rise Residential Structures Subjected to Blast Vibrations*, M.S. Thesis, Northwestern University, Dept. of Civil Engineering.
- Pierce, W. E., and S. V. Crum, 1996, *Assessment of Low-Frequency Blast Vibrations and Potential Impacts on Structures*, Report to the Office of Surface Mining EF68-IA 92-12180, 22 pp.
- Seaquist, E. O., 1980, *Diagnosing and Repairing House Structure Problems*, Professional Equipment Publications, West Babylon, NY, 255 pp.
- Siskind, D. E., V. J. Stachura, M. S. Stagg and J. W. Kopp, 1980a, *Structure Response and Damage Produced by Airblast from Surface Mining*, Bureau of Mines RI 8485, 111 pp.
- Siskind, D. E., M. S. Stagg, J. W. Kopp and C. H. Dowding, 1980b, *Structure Response and Damage Produced by Ground Vibration from Surface Mine Blasting*, Bureau of Mines RI 8507, 74 pp.
- Siskind, D. E., 1986, *Rock Blasting and Environmental Impacts*, Unpublished.
- Siskind, D. E., S. V. Crum, R. E. Otterness and J. W. Kopp, 1989, *Comparative study of Blasting Vibrations from Indiana Surface Coal Mines*, Bureau of Mines RI 9226, 40 pp.

- Siskind, D. E., S. V. Crum and M. N. Plis, 1993, *Blast Vibrations and Other Potential Causes of Damage in Residences Near a Large Surface Coal Mine in Indiana*, BuMines RI 9455, 62 pp.
- Siskind, D. E., M. S. Stagg, W. E. Pierce and S. V. Crum, 1996, *Low Frequency Blast Vibrations at a High Water Table Site*, Proceedings of the 22nd Annual Conference on Explosives and Blasting Technique, Society of Explosives Engineers, Orlando, FL.
- Stagg, M. S., D. E. Siskind, M. G. Stevens and C. H. Dowding, 1984, *Effect of Repeated Blasting on a Wood-Frame House*, Bureau of Mines RI 8896, 82 pp.
- White, T., R. Farnfield and M. Kelly, 1993, *The Effects of Surface Mine Blasting on Buildings*, Proc. from the Fourth Intl. Symp. on Rock Fragmentation by Blasting, Vienna, Austria, pp. 105-111.

Table 1. House Descriptions

Name	General Location (Closest Mine)	General Construction	Approx. 1st Floor Square Footage	Natural Frequency [‡]	Comments	Other Reference
Lhemkuhler	Southwestern, IN (Phoenix)	Older 1- story wood frame.	1800	7 Hz	Oak frame, wood exterior, high pitched roof, full basement, good condition, occasionally occupied.	Crum and Pierce (1995)
Shack	West-central, IN (Amax)	Older 1- story wood frame.	750	5.5 Hz	Wood exterior, no basement, closest home to blasting, poor condition, abandoned.	Crum and Pierce (1995), Pierce and Crum (1996)
Smith	West-central, IN (Amax)	Older 1- story wood frame.	1400	6 Hz	Wood exterior, no basement, fair condition, occupied.	None prior to this report
Arvida	Southeastern, FL (+)	New 1-story cement block.	2500	11 Hz, highest corner (11-ft ceilings)	Vertical reinforcement, poured concrete foundation slab, no basement, complicated floor plan with many corners and angles and different ceiling heights, new condition, unoccupied.	Siskind et al (1996)
Jordan	West-central, PA (C&K)	Older 3- story wood frame.	950	~ 6 Hz	Remodeled older farmhouse, brick exterior and slate roof, good condition, occupied.	Crum and Pierce, (1995)
McConnell	West-central, PA (C&K)	Modern 2- story wood frame.	2000	Not Determined	Newer home located near Jordan house inspected for blast-related cracking but was not instrumented for response, occupied.	Crum and Pierce (1995)
Hoover	Southwestern, IN (Amax)	Older 2- story wood frame.	2000	~ 5-6 Hz	Remodeled farmhouse with newer additions, high pitched slate roof, wood siding, good condition, occupied.	Crum and Siskind, (1993)
Hole	West-central, IN (Amax)	Older 1- story wood frame.	1000	5 Hz	Abandoned home in very poor condition located close to blating area, appears to have been damaged by heavy equipment during removal of top soil.	None prior to this report
Manor	West-central, IN (Amax)	Older 1- story wood frame.	1200	5-6 Hz	Similar construction and response characteristics to the Shack described above, abandoned.	None prior to this report.
Pritcher	West-central, IN (Amax)	Older 1- story wood frame.	2000	5 Hz	Similar construction and response characteristics as the Smith house described above, occupied.	None prior to this report

* All the homes were being subjected to blast vibrations from surface coal-mine overburden blasting, except for the Arvida house which was near smaller-diameter quarry-type blasting at a high water table site.

‡ The natural frequency was determined as the average of several natural frequency values found from high corner structure response recordings. Natural frequencies were determined from the peak amplitude frequency component of the Fourier frequency spectra except for the Jordan and Hoover homes where time-history period inversion methods were used.

+ The Arvida house was located in a land development site. Blasting for excavation and fill was being subcontracted on site.

Table 2. Blast, Ground Vibration and Crack-Inspection Information

Name	Number of Monitored Blasts	Number of Blasts with Crack Inspections (Number of Inspection Sites in Home)	Number of Blasts Within Range of Peak Particle Velocities (Number of Blasts with Crack Inspections)			
			<0.5 in/s	0.5-0.99 in/s	1.0-4.99 in/s	>5.0 in/s
Lhemkuhler	106	7 (10)	33	36 (4)	36 (3)	1 (0)
Shack	35	35 (7)	8 (8)	8 (8)	15 (15)	4 (4)
Smith	20	0	8	10	2	0
Arvida	11	0	11	0	0	0
Jordan	4	4 (4)	4 (4)	0	0	0
McConnell*	4	4 (5)	4 (4)	0	0	0
Hoover	5	0	5	0	0	0
Manor	5	0	3	2	0	0
Hole	9	0	1	1	7	0
Pritcher	2	0	1	1	0	0

* The same events were monitored at the McConnell and Jordan homes which were about the same distance from the blasting. The McConnell house was not instrumented for structure response but pre- and post-blast crack inspections were made.

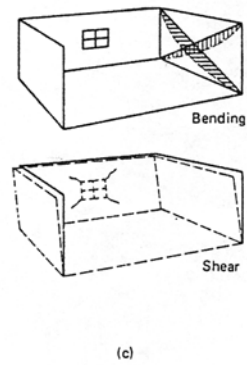
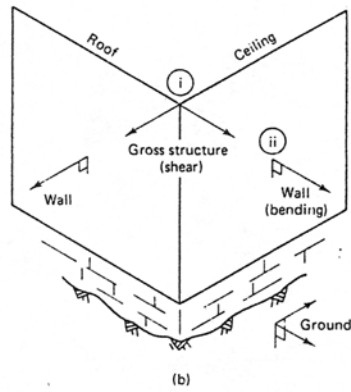
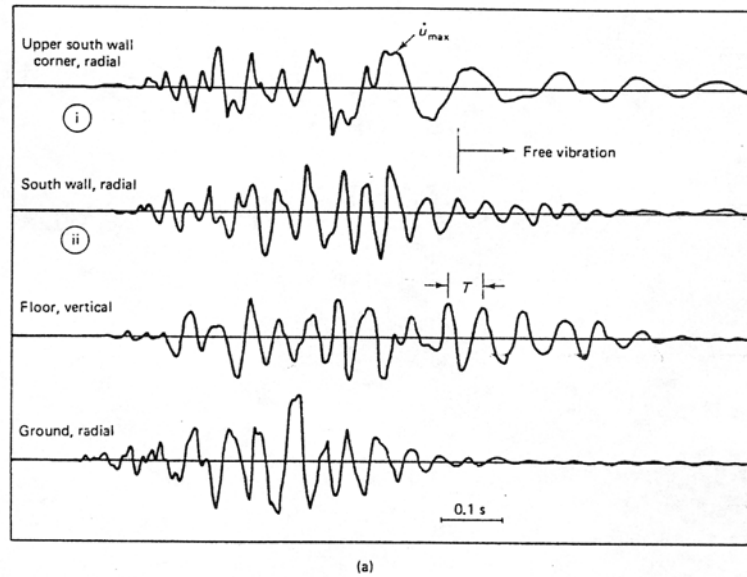


Figure 1. Measurement of superstructure and wall response: (a) motions; (b) transducer placement (i and ii) and direction sensitivity; (c) diagrams of response motions (after Dowding, 1985).

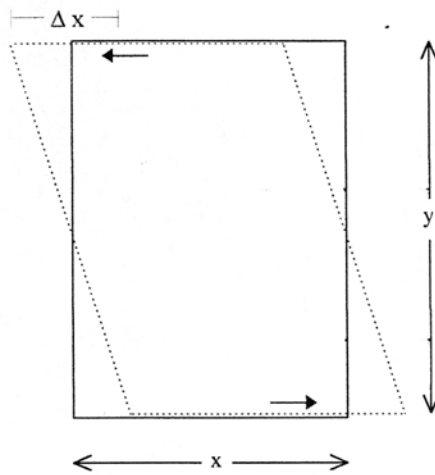


Figure 2. Diagram of global angular distortion of a planar body. Parameters are identified in the text.

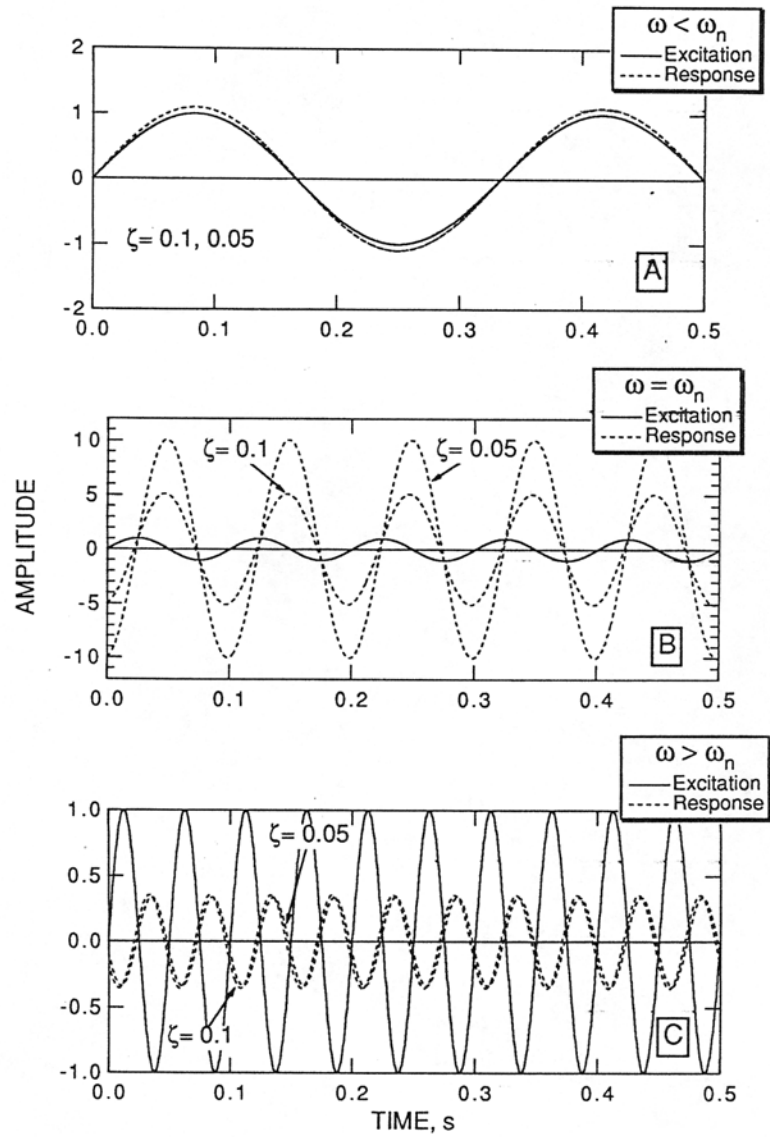
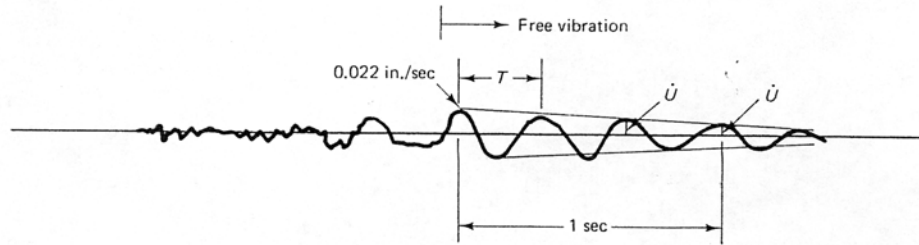


Figure 3. Single-degree-of-freedom response for infinitely long, continuous, harmonic, sinusoidal excitation and unit amplitude excitation for damping values of 5 and 10 pct. A: Excitation frequency at 1/3 the system natural frequency; B: excitation frequency equal to the natural frequency and C: excitation frequency at 2-times the natural frequency.



$$T = \text{damped period} = \frac{2\pi}{\rho_d}$$

$$\beta = \frac{1}{2\pi} \left(-\ln \frac{\dot{u}_{n+1}}{\dot{u}_n} \right), \quad \rho = \rho_d \sqrt{1 - \beta^2} = \rho_d, \text{ for small } \beta \text{ values}$$

Figure 4. Example structure response recording showing period of assumed free-vibration response (T), and calculation of damping and (after Dowding, 1985).

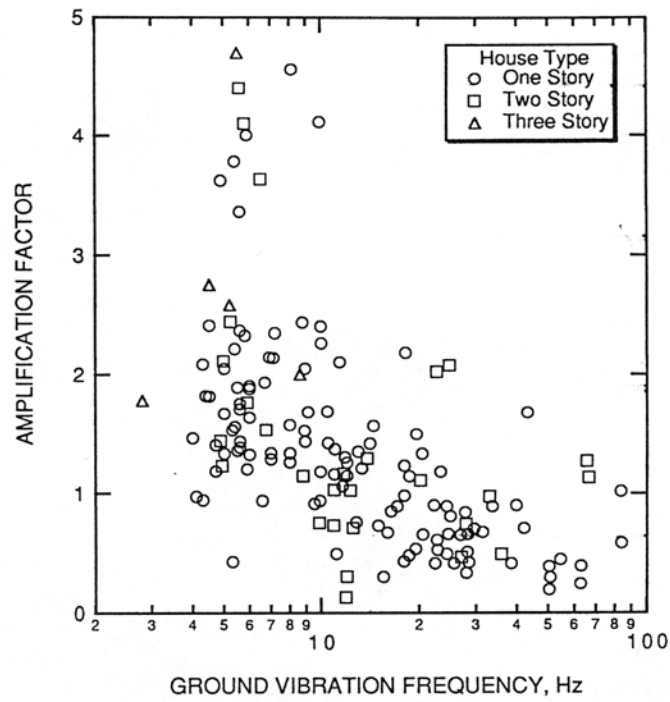


Figure 5. Recent and historical Bureau of Mines measurements of amplification factor versus ground vibration frequency.

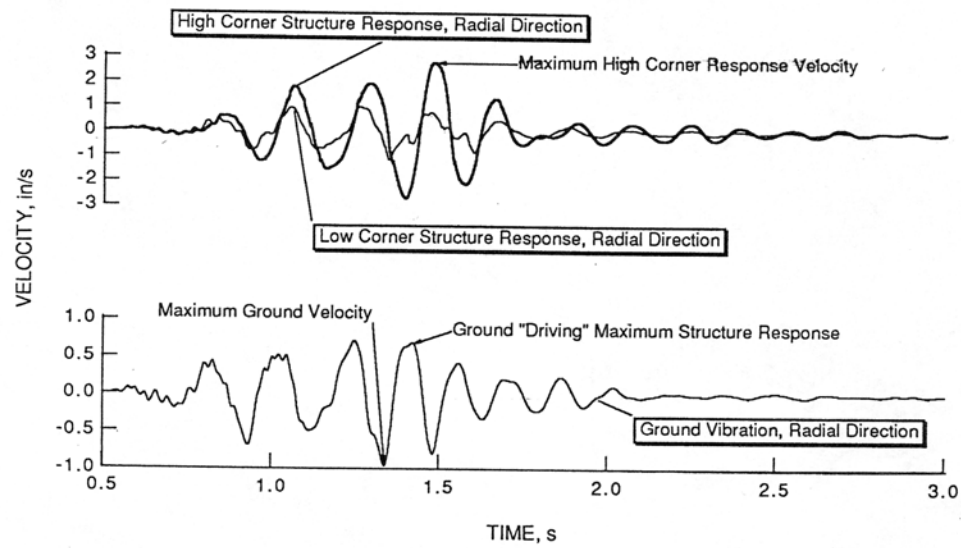


Figure 6. Example ground vibration and low and high corner structure response measurements at the Shack. Temporal relationships are indicated between maximum ground vibration velocity, driving ground vibration velocity and maximum high corner response velocity.



Figure 7. The Shack (abandoned), located at the Amax mine in west-central Indiana.



Figure 8. The Manor (abandoned), located at the Amax mine in west-central Indiana.



Figure 8b. The Hemkeahler House.



Figure 9. The Pritchett house, located near the Amax mine in west-central Indiana.



Figure 10. The Smith house, located near the Amax mine in central Indiana.



Figure 11. The Hoover house, located several miles from the Amax in southwestern Indiana



Figure 12. The Jordan house, located near the C&K mine in west-central Pennsylvania.



Figure 13. The McConnell house, located near the C&K mine in west-central Pennsylvania.



Figure 14. The Mini-Seis Seismograph.



Figure 15. Shallow-burial installation of the Mini-Seis ground vibration transducer. Before monitoring, the geophone was covered with soil, lightly tamped around the edges and top.

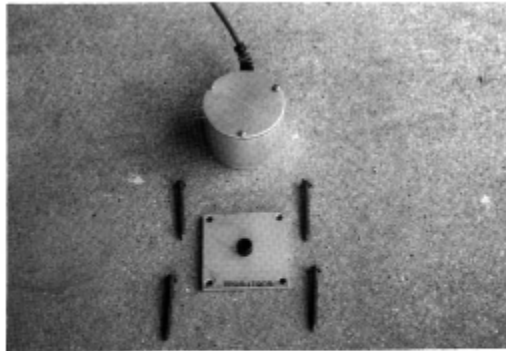


Figure 16. The Mini-Seis transducer and custom structural mounting hardware.



Figure 17. Transducer installed for high corner structural monitoring at the Shack.

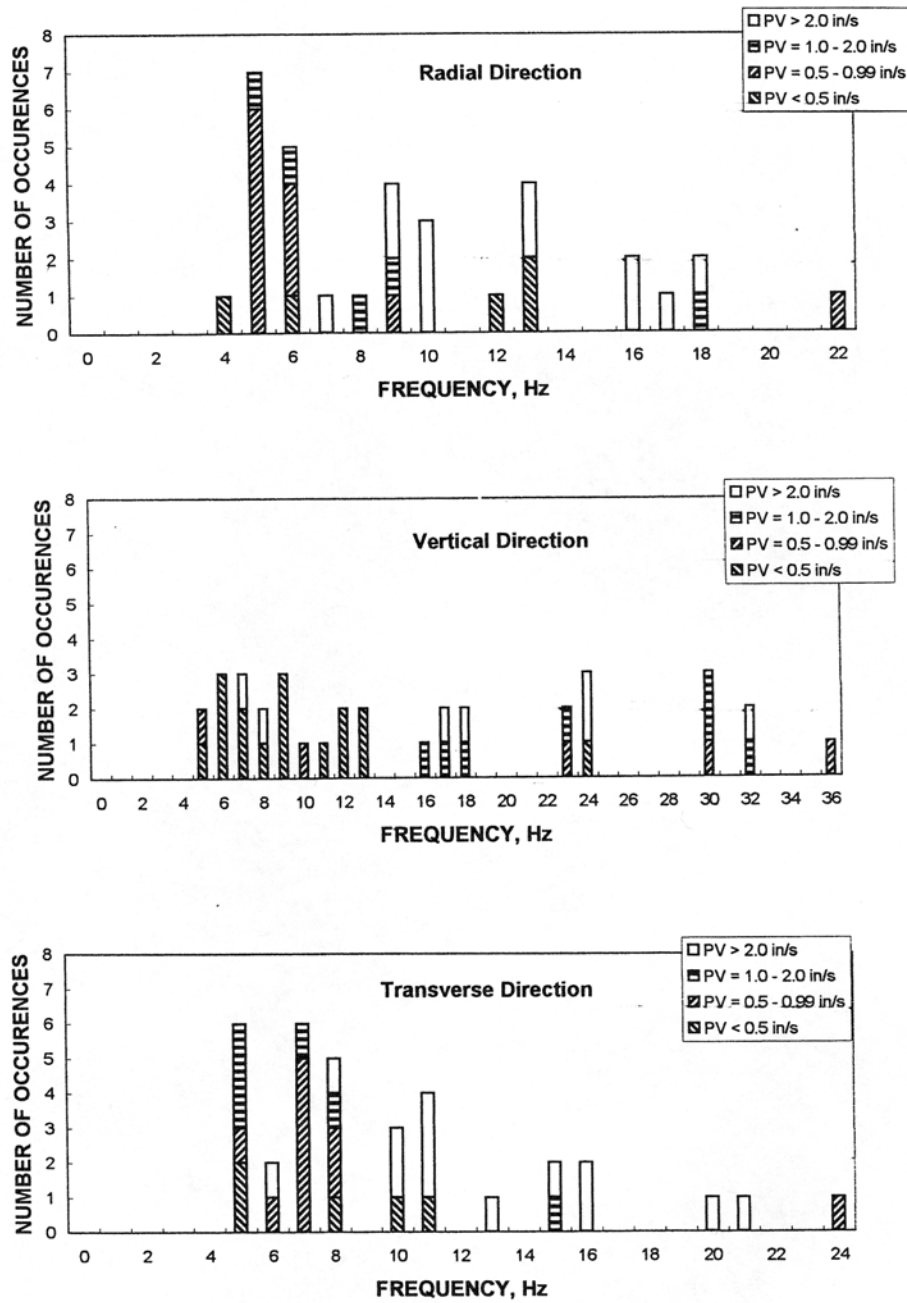


Figure 18. Histogram of frequencies associated with maximum ground vibration monitored at the Shack. Particle velocity (PV) amplitudes are indicated in 1 in/s intervals.

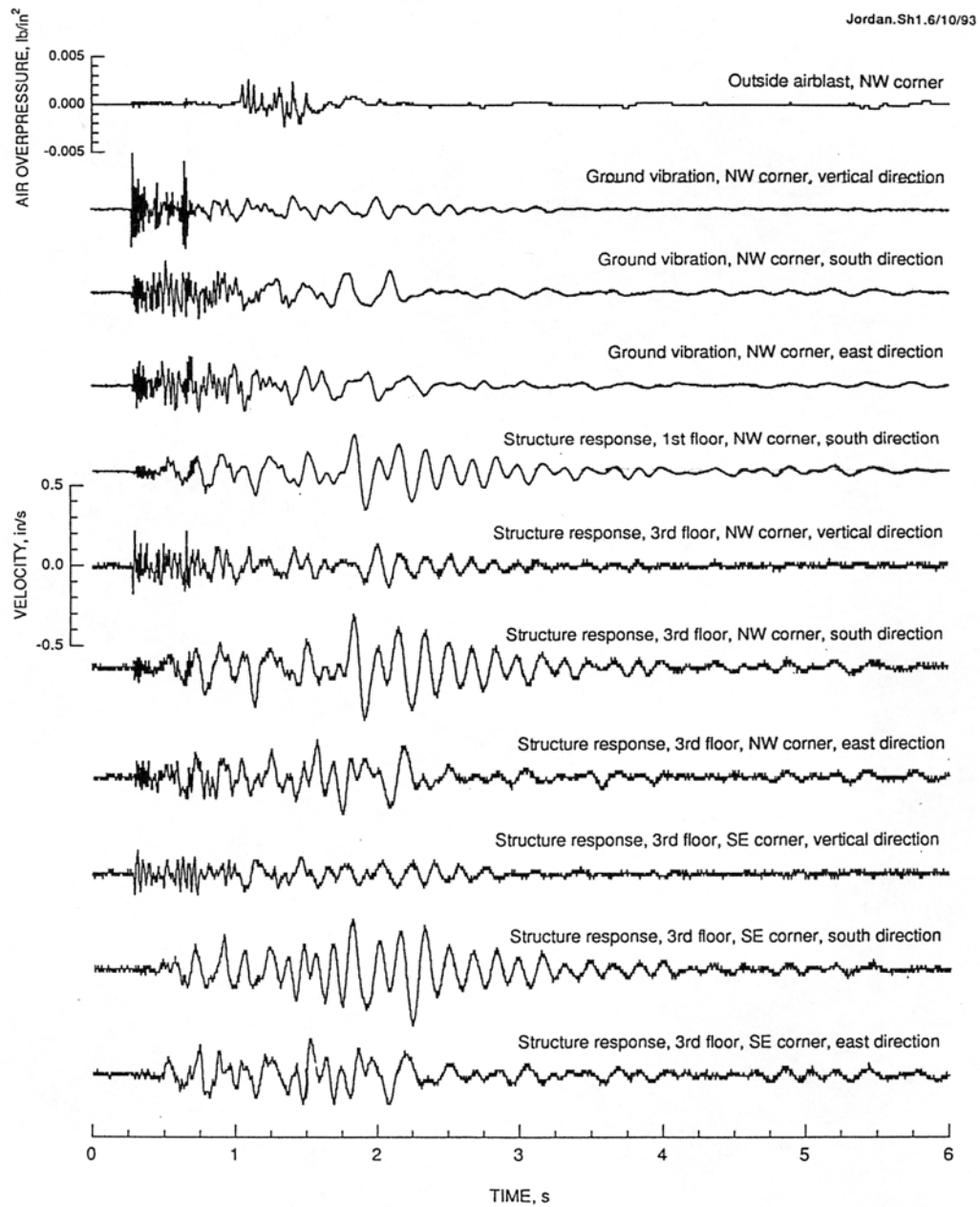


Figure 19. Ground vibrations, airblast and structure response measured at the Jordan house on 6/10/93.

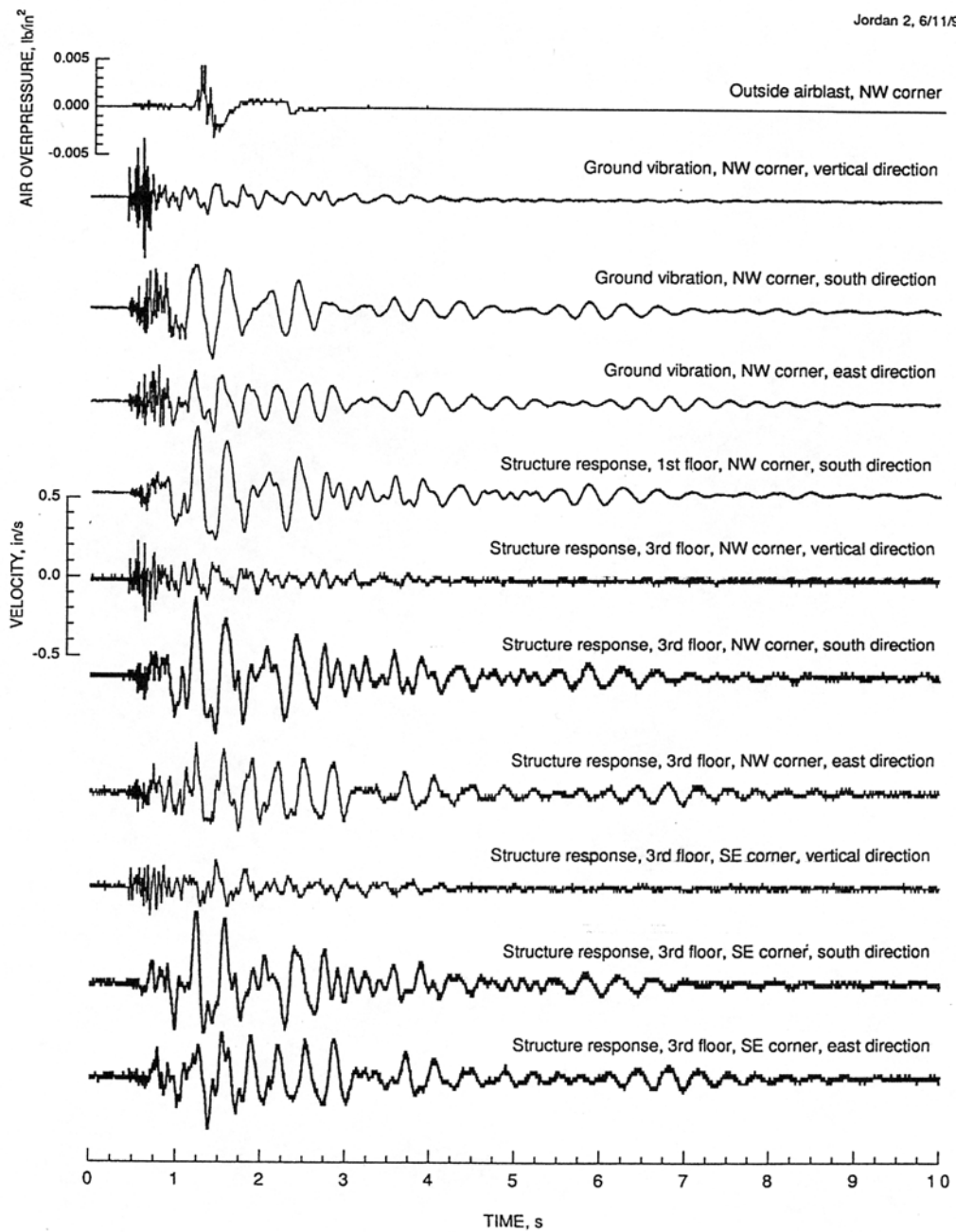


Figure 20. Ground vibration, airblast and structure response measured at the Jordan house on 6/11/93.

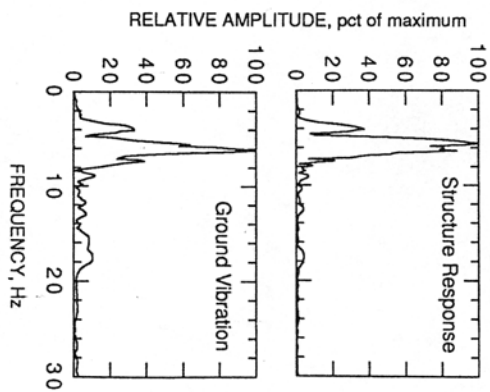
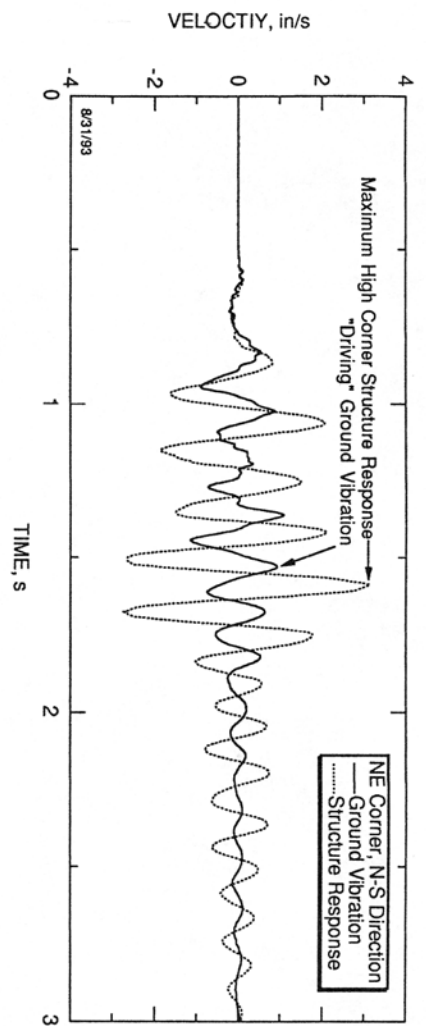


Figure 21. Ground vibration and structure response recorded at the Shack. The corresponding Fourier frequency spectra is shown to the right of the time histories. The record is an excellent example of structure response to ground vibration at the structural natural frequency: note the similarity in the frequency spectra between the ground vibration and structure response.

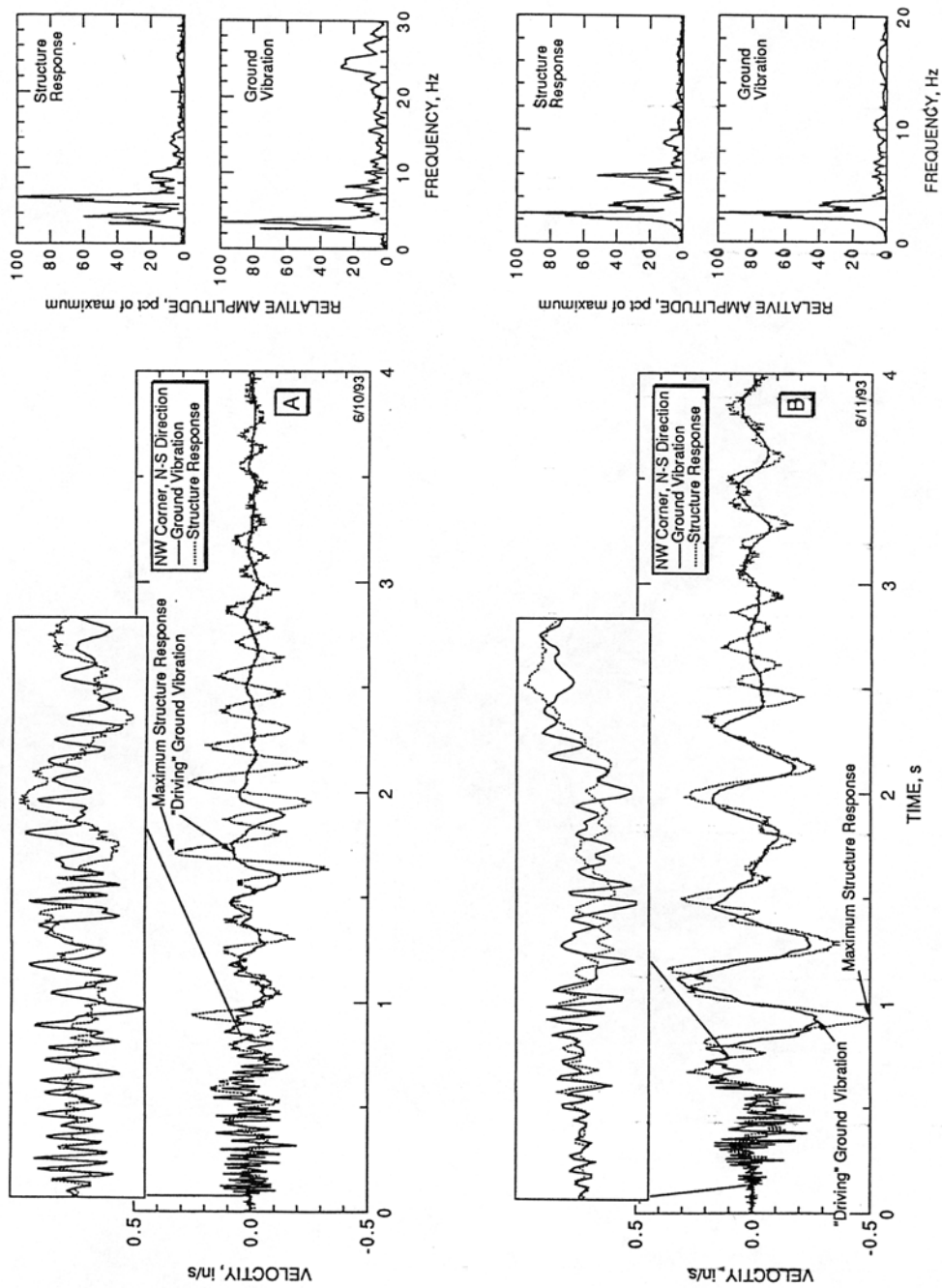


Figure 22. Ground vibration, structure response and Fourier frequency spectra for two shots recorded at the Jordan house. The inset shows the high frequency portion of the vibrations at an expanded scale. Figure 22A shows some natural frequency response while figure 22B exemplifies response to ground vibration frequencies below the natural frequency.

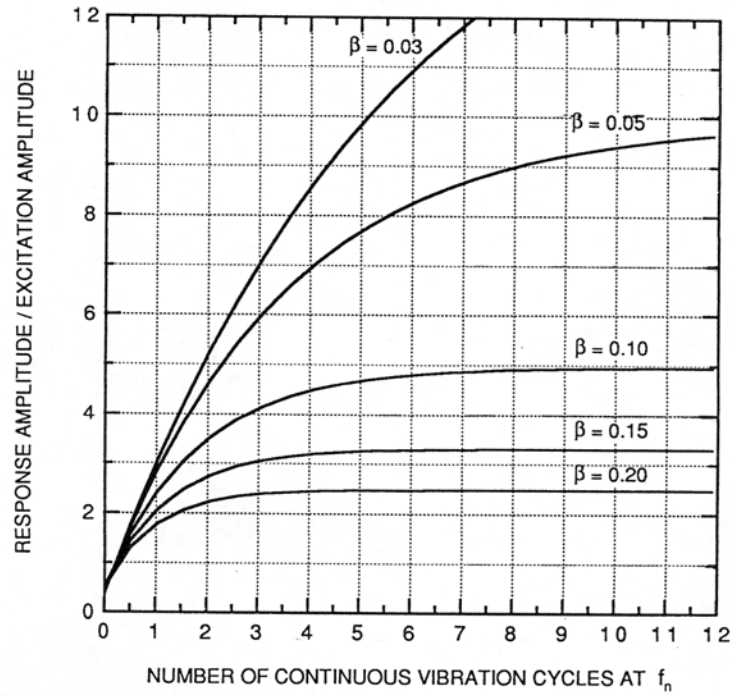


Figure 23. Amplification versus number of continuous excitation cycles at the structural natural frequency using the finite-duration Duhamel-pseudovelocity model (equations 3 and 4).

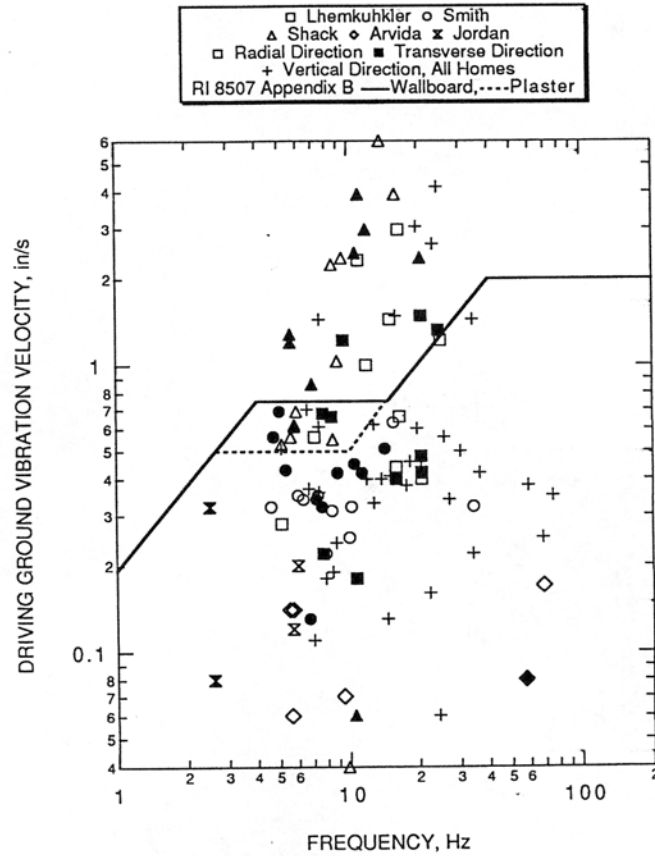


Figure 24. Driving ground vibration velocity versus frequency for the representative data set described in the text plotted with the RI 8507 Appendix B blast level chart. Radial and transverse measurements are denoted by open and closed house symbols, respectively. Vertical component measurements correspond to all homes.

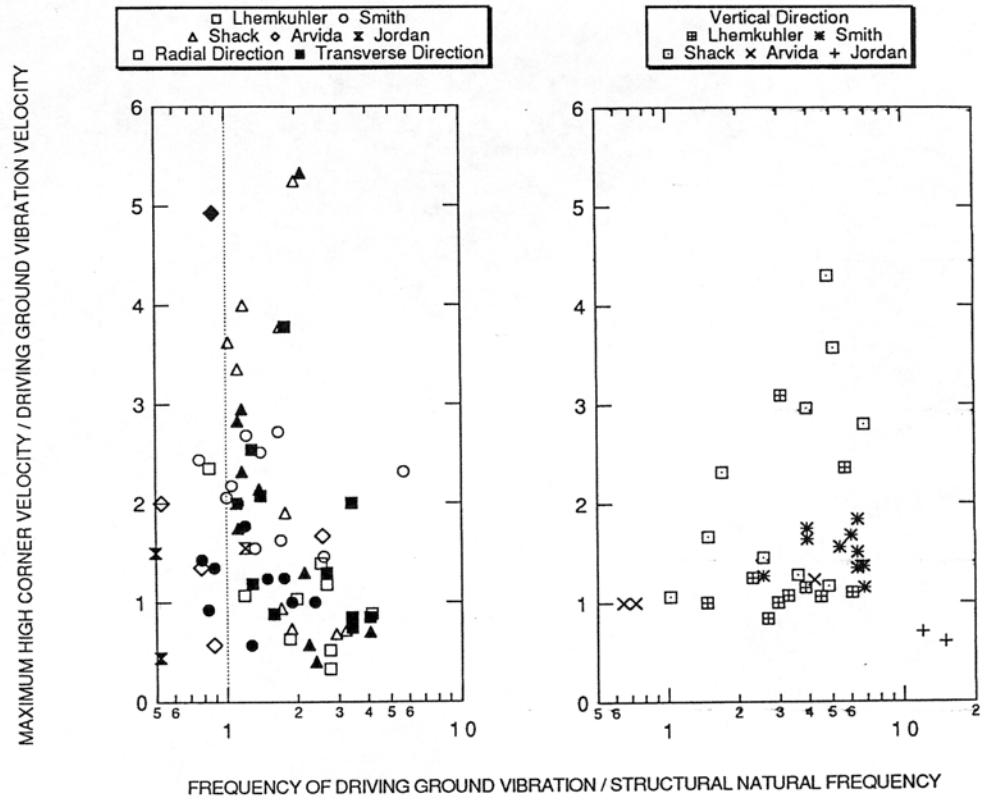


Figure 25. Amplification factor versus frequency ratio from monitoring at the test houses. Amplification was computed as the maximum high corner structure response velocity divided by driving ground vibration velocity. Frequency ratio is the ground vibration frequency divided by the structural natural frequency (determined from horizontal components of motion). The determination of natural frequency is discussed in the text and the values for the individual homes are listed in table 1.

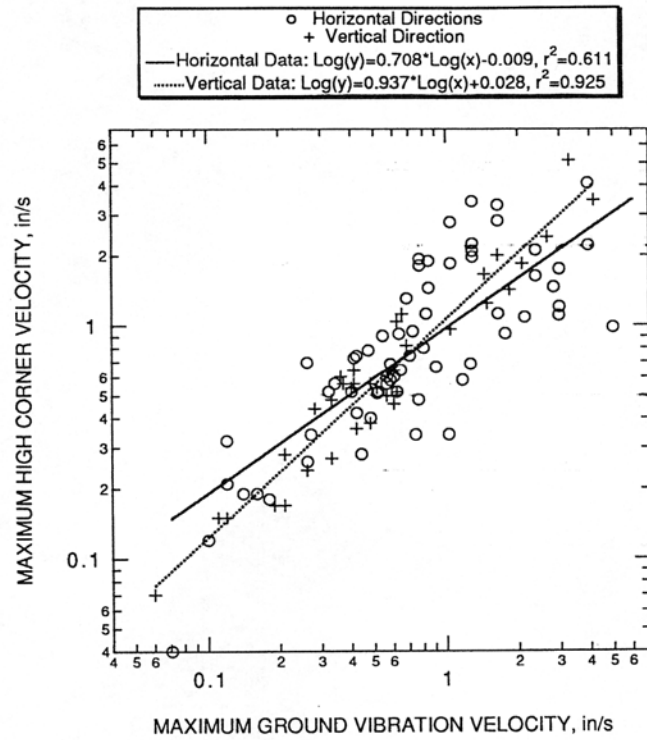


Figure 26. Maximum high corner structure response velocity versus maximum ground vibration velocity. All statistics were performed on log-transformed data.

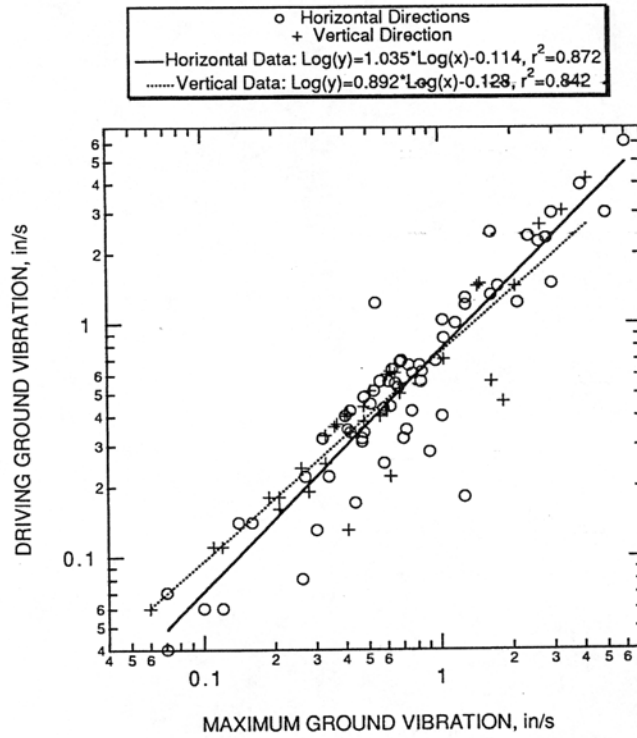


Figure 27. Driving ground vibration velocity versus maximum ground vibration velocity. All statistics were performed on log-transformed data.



Figure 28. Visual inspections for cracking at the Shack. A 7-power optical magnifier and sidelight are being used. Preexisting cracks before the study were highlighted with marker.



Figure 29. Visual inspections for cracking at the Lhemkuher house showing the optical magnifier and 100 watt sidelight.

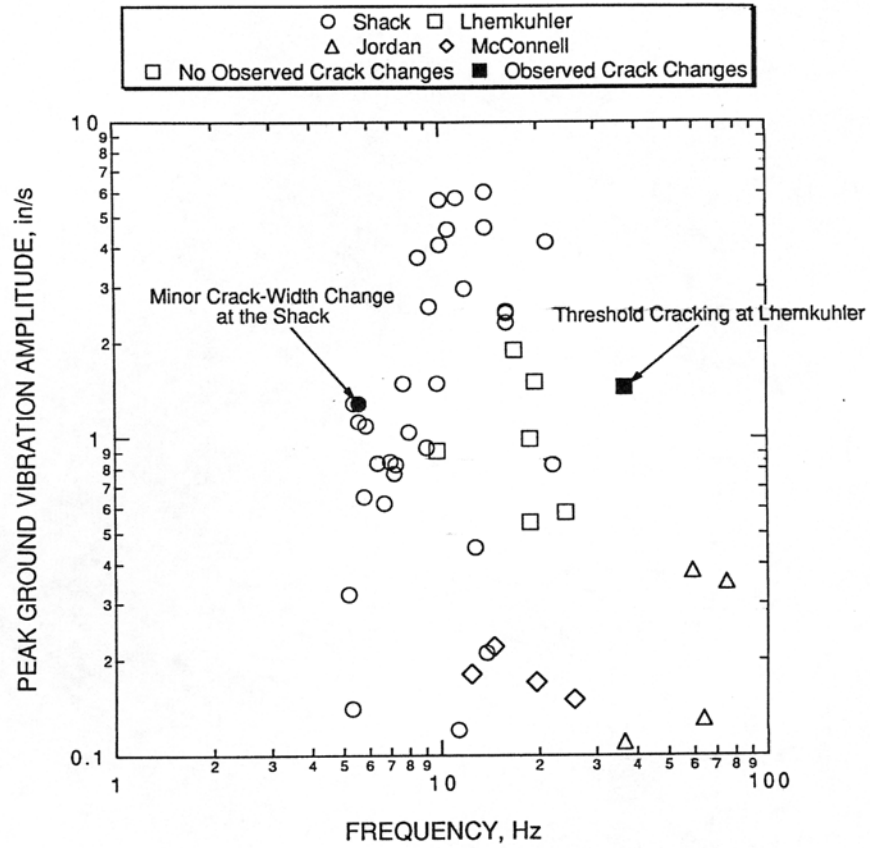


Figure 30. Cracking and non-cracking observations at the test houses plotted as a function of peak ground vibration amplitude versus frequency.

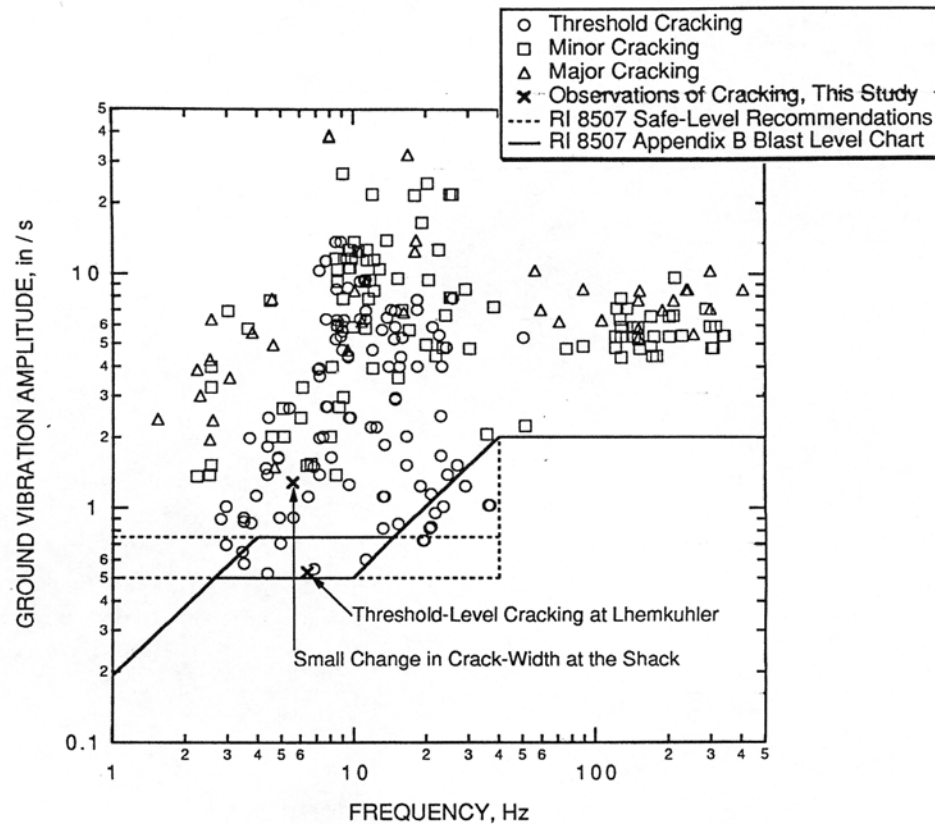


Figure 31. Observations of cracking reported in this study (indicated with an "x") plotted as a function of driving ground vibration velocity versus frequency, along with cracking observations and safe-level recommendations from RI 8507. Driving ground vibration is used here (as opposed to peak amplitudes in figure 30) to be consistent with the analysis methods incorporated in the RI 8507 study.

APPENDIX A: DATA TABLES

Table A-1: Lhemkuhler House

Radial Direction (Parallel to Major Roof Line)										
Shot Date	Time *	Maximum Ground Vibration, $V_G(t_1)$ in/s	Frequency, Hz	Driving Ground Vibration, $V_G(t_2)$ in/s	Frequency, Hz	Maximum High Corner Structure Response, $V_{High}(t_3)$ in/s	Frequency, Hz	Corresponding Low Corner Structure Response, $V_{Low}(t_3)$ in/s	Frequency, Hz	Maximum High-Low Differential Displacement, in
5-18-94	1320	-0.56	7.1	-0.56	7.1	-0.60	6.2	-0.36	6.4	0.004
5-26-94	1558	-1.02	24.3	-0.40	20.5	0.34	16.0	-0.06	42.7	0.004
5-27-94	1531	-4.96	21.3	-2.96	16.5	-0.98	12.4	0.26	16.0	-0.015
5-31-94	1416	-0.74	19.6	0.66	16.5	0.34	12.1	-0.06	13.1	0.005
6-3-94	1551	-1.76	19.6	1.44	15.1	0.92	10.2	-0.18	14.2	0.012
6-8-94	1550	-1.16	17.6	1.00	11.9	0.58	11.1	0.28	11.1	0.004
6-9-94	1535	2.80	18.2	-2.32	11.1	-1.46	5.6	-0.08	4.4	-0.013
7-13-94	1029	-0.90	21.3	0.28	5.1	0.66	7.1	0.34	6.2	0.006
7-18-94	1555	2.12	17.0	-1.22	24.9	-1.08	16.5	-0.26	21.3	-0.009
7-19-94	1200	-0.62	15.5	0.44	16.0	-0.52	10.2	-0.02	10.0	-0.005

Vertical Direction										
Shot Date	Time *	Maximum Ground Vibration, $V_G(t_1)$ in/s	Frequency, Hz	Driving Ground Vibration, $V_G(t_2)$ in/s	Frequency, Hz	Maximum High Corner Structure Response, $V_{High}(t_3)$ in/s	Frequency, Hz	Corresponding Low Corner Structure Response, $V_{Low}(t_3)$ in/s	Frequency, Hz	Maximum High-Low Differential Displacement, in†
5-18-94	1320	0.26	34.1	0.24	8.8	0.24	12.8	0.24	12.1	low
5-26-94	1558	0.60	42.6	-0.42	36.5	-0.46	30.1	-0.44	30.1	low
5-27-94	1531	2.64	23.2	2.64	23.2	2.40	23.2	2.32	23.2	0.001
5-31-94	1416	0.56	15.0	-0.40	13.8	-0.50	13.1	-0.48	13.1	low
6-3-94	1551	0.62	21.3	0.22	34.1	0.52	25.6	0.52	25.6	low
6-8-94	1550	0.60	19.6	0.60	19.6	0.64	16.5	0.64	16.5	low
6-9-94	1535	1.48	16.0	1.48	16.0	1.24	23.2	1.24	22.2	low
7-13-94	1029	0.48	36.5	-0.38	17.7	0.38	28.4	-0.38	26.9	low
7-18-94	1555	1.84	28.4	-0.46	18.3	1.42	23.2	-1.4	24.2	-0.001
7-19-94	1200	0.42	32.0	-0.34	27.0	-0.36	21.3	-0.38	12.4	0.002

Transverse Direction (Perpendicular to Major Roof Line)										
Shot Date	Time *	Maximum Ground Vibration, $V_G(t_1)$ in/s	Frequency, Hz	Driving Ground Vibration, $V_G(t_2)$ in/s	Frequency, Hz	Maximum High Corner Structure Response, $V_{High}(t_3)$ in/s	Frequency, Hz	Corresponding Low Corner Structure Response, $V_{Low}(t_3)$ in/s	Frequency, Hz	Maximum High-Low Differential Displacement, in
5-18-94	1320	0.34	11.1	0.22	7.7	0.56	7.1	0.22	7.2	0.007
5-26-94	1558	0.48	20.4	0.48	20.4	0.40	9.6	0.06	8.7	0.006
5-27-94	1531	2.96	16.0	1.48	20.5	-1.10	5.8	-0.14	8.7	-0.028
5-31-94	1416	0.40	16	-0.40	16.0	0.52	10.0	0.52	10	0.004
6-3-94	1551	0.82	8.5	0.66	8.4	1.12	7.5	0.52	7.1	0.012
6-8-94	1550	0.76	12.1	-0.42	20.5	0.48	8.0	0.14	8.0	0.007
6-9-94	1535	-1.64	16.0	1.32	24.4	1.12	9.4	0.50	8.1	0.009
7-13-94	1029	0.68	7.7	0.68	7.7	1.30	6.9	0.78	6.7	0.011
7-18-94	1555	-1.26	12.4	0.18	10.7	0.68	8.5	0.28	7.3	0.007
7-19-94	1200	0.54	8.9	0.22	9.5	0.90	7.4	0.40	6.4	0.009

* Times are approximate.

† "low" indicates that the absolute value is less than 0.001 in.

Table A-2: The Shack

Radial Direction (Parallel to Major Roof Line)										
Shot Date	Time *	Maximum Ground Vibration, $ V_G(t_i) $ in/s	Frequency, Hz	Driving Ground Vibration, $V_G(t_i)$ in/s	Frequency, Hz	Maximum High Corner Structure Response, $V_{High}(t_i)$ in/s	Frequency, Hz	Corresponding Low Corner Structure Response, $V_{Low}(t_i)$ in/s	Frequency, Hz	Maximum High-Low Differential Displacement, in
10-12-93	1236	0.65	6.6	0.55	8.5	2.08	5.3	0.71	6.2	0.044
10-12-93	1412	0.07	13.8	0.04	9.8	-0.21	7.1	-0.07	6.3	-0.003
10-13-93	1415	0.67	5.3	-0.53	5.1	-1.92	4.9	-0.34	4.2	-0.013
10-14-93	1422	0.96	5.9	0.69	5.9	2.76	5.5	0.63	5.1	0.020
10-14-93	1438	0.83	6.0	0.56	5.6	1.88	5.3	0.53	5.8	0.042
6-1-94	1722	2.60	9.3	-2.24	8.5	-2.1	5.0	-1.26	7.5	-0.040
6-1-94	1731	2.36	9.4	2.36	9.4	1.74	4.8	0.82	10.6	0.045
7-27-94	1651	1.03	8.9	-1.03	8.9	-1.96	5.5	-0.23	8.8	-0.053
8-23-94	1749	6.00	13.8	-6.00	13.8	-4.08	4.5	-1.28	13.9	-0.130
8-23-94	1812	3.92	16.0	3.92	16.0	2.80	6.5	0.94	10.0	0.054

Vertical Direction										
Shot Date	Time *	Maximum Ground Vibration, $ V_G(t_i) $ in/s	Frequency, Hz	Driving Ground Vibration, $V_G(t_i)$ in/s	Frequency, Hz	Maximum High Corner Structure Response, $V_{High}(t_i)$ in/s	Frequency, Hz	Corresponding Low Corner Structure Response, $V_{Low}(t_i)$ in/s	Frequency, Hz	Maximum High-Low Differential Displacement, in†
10-12-93	1236	0.36	74	-0.36	7.4	0.06	7.1	0.55	6.7	low
10-12-93	1412	0.06	24.3	-0.06	24.3	-0.07	22.2	-0.07	22.2	low
10-13-93	1415	0.28	6.1	-0.19	8.5	0.44	0.4	7.5	7.5	0.001
10-14-93	1422	0.33	12.8	-0.33	12.8	0.48	10.8	0.48	6.6	-0.005
10-14-93	1438	0.51	5.1	-0.51	5.1	-0.54	7.6	-0.58	7.4	0.001
6-1-94	1722	1.64	30.1	-0.56	25.6	2.00	11.9	2.02	12.8	0.002
6-1-94	1731	2.08	32.0	1.44	34.2	1.84	30.1	1.90	30.1	low
7-27-94	1651	0.52	10.6	0.13	14.6	0.56	9.3	0.4	11.9	0.004
8-23-94	1749	4.16	24.3	-4.16	24.3	3.44	15.1	2.96	15	0.005
8-23-94	1812	4.40	30.1	2.96	15.0	-5.12	204	-5.20	20.4	low

Transverse Direction (Perpendicular to Major Roof Line)										
Shot Date	Time *	Maximum Ground Vibration, $ V_G(t_i) $ in/s	Frequency, Hz	Driving Ground Vibration, $V_G(t_i)$ in/s	Frequency, Hz	Maximum High Corner Structure Response, $V_{High}(t_i)$ in/s	Frequency, Hz	Corresponding Low Corner Structure Response, $V_{Low}(t_i)$ in/s	Frequency, Hz	Maximum High-Low Differential Displacement, in
10-12-93	1236	1.28	5.6	1.28	5.6	2.24	5	-0.40	8.0	-0.008
10-12-93	1412	0.12	11.3	0.06	10.5	0.32	6.3	0.10	5.6	0.005
10-13-93	1415	0.77	7.2	0.61	5.8	1.8	5.3	-0.20	10.0	0.057
10-14-93	1422	1.04	8.0	0.86	6.9	1.84	5.2	0.11	17.7	0.055
10-14-93	1438	0.84	7.0	0.62	5.8	1.44	5.4	0.02	13.5	0.042
6-1-94	1722	2.36	20.4	-2.36	20.4	1.62	4.9	0.88	22.3	0.006
6-1-94	1731	2.96	11.9	2.96	11.9	-1.20	6.7	1.22	11.9	-0.045
7-27-94	1651	1.28	5.4	-1.2	5.6	-3.40	4.6	-0.70	4.6	-0.094
8-23-94	1749	3.92	11.1	-3.9	11.1	-2.20	4.4	-0.10	8.5	-0.080
8-23-94	1812	4.64	13.8	-2.5	10.7	3.28	5.7	-0.80	14.2	0.101

* Times are approximate.

† "low" indicates that the absolute value is less than 0.001 in.

Table A-3: Smith House

Radial Direction (Parallel to Major Roof Line)										
Shot Date	Time *	Maximum Ground Vibration, $ V_G(t_1) $ in/s	Frequency, Hz	Driving Ground Vibration, $V_G(t_2)$ in/s	Frequency, Hz	Maximum High Corner Structure Response, $V_{High}(t_3)$ in/s	Frequency, Hz	Corresponding Low Corner Structure Response, $V_{Low}(t_3)$ in/s	Frequency, Hz	Maximum High-Low Differential Displacement, in
5-4-94	1249	0.32	10.2	-0.32	10.2	-0.52	8.9	0.00	10.2	-0.009
5-5-94	1247	0.27	13.4	-0.22	7.9	-0.34	9.6	-0.15	7.9	-0.003
5-5-94	1431	0.70	25.6	0.32	34.2	0.74	28.4	-0.57	25.5	0.008
5-9-94	1436	0.58	22.2	0.25	10.0	0.68	18.9	-0.18	10.0	0.009
5-10-94	1040	0.63	15.5	0.63	15.5	0.92	6.8	0.02	15.5	0.021
5-11-94	1001	0.72	22.2	-0.35	7.3	-0.94	7.4	-0.22	7.3	-0.015
5-12-94	0939	0.47	15.5	0.31	8.4	0.78	7.5	0.28	8.4	0.011
5-13-96	1316	0.42	8.1	-0.34	6.3	-0.74	6.7	-0.33	6.3	-0.009
5-13-94	1323	0.47	11.9	0.32	4.6	0.78	5.9	0.12	4.6	0.017
5-17-94	1327	0.41	8.9	-0.35	6	-0.72	6.5	-0.34	6.0	-0.009

Vertical Direction										
Shot Date	Time *	Maximum Ground Vibration, $ V_G(t_1) $ in/s	Frequency, Hz	Driving Ground Vibration, $V_G(t_2)$ in/s	Frequency, Hz	Maximum High Corner Structure Response, $V_{High}(t_3)$ in/s	Frequency, Hz	Corresponding Low Corner Structure Response, $V_{Low}(t_3)$ in/s	Frequency, Hz	Maximum High-Low Differential Displacement, in†
5-4-94	1249	0.56	32.0	-0.37	32.0	-0.56	32.0	-0.02	32	-0.003
5-5-94	1247	0.21	24.3	0.16	19.7	0.28	24.4	0.10	19.7	0.001
5-5-94	1431	1.44	34.1	1.44	34.1	1.66	30.1	-0.55	36.8	0.011
5-9-94	1436	1.04	36.5	0.70	34.0	0.96	30.1	-0.10	34	0.005
5-10-94	1040	0.65	30.1	0.61	32.1	1.12	30.1	-0.01	32.1	0.006
5-11-94	1001	0.62	30.1	-0.62	30.1	1.04	21.3	0.03	30.1	0.008
5-12-94	0939	0.68	18.2	-0.50	19.7	0.82	22.2	-0.11	19.7	0.007
5-13-96	1316	0.40	32	-0.40	32.0	0.54	21.3	-0.01	32.0	0.004
5-13-94	1323	0.41	11.9	-0.41	26.9	-0.64	18.2	-0.10	26.9	-0.005
5-17-94	1327	0.48	28.4	-0.44	12.8	-0.56	18.9	-0.15	12.8	-0.003

Transverse Direction (Perpendicular to Major Roof Line)										
Shot Date	Time *	Maximum Ground Vibration, $ V_G(t_1) $ in/s	Frequency, Hz	Driving Ground Vibration, $V_G(t_2)$ in/s	Frequency, Hz	Maximum High Corner Structure Response, $V_{High}(t_3)$ in/s	Frequency, Hz	Corresponding Low Corner Structure Response, $V_{Low}(t_3)$ in/s	Frequency, Hz	Maximum High-Low Differential Displacement, in
5-4-94	1249	0.32	7.6	0.32	7.6	0.18	6.3	0.30	7.6	-0.002
5-5-94	1247	0.30	8.9	0.13	6.7	-0.26	4.1	0.22	8.9	-0.014
5-5-94	1431	0.69	5.0	0.69	5.0	-0.64	4.9	0.25	5.0	-0.029
5-9-94	1436	0.53	10.8	-0.51	14.2	0.51	7.0	0.01	14.2	0.011
5-10-94	1040	0.42	11.3	-0.42	11.3	0.42	8.3	-0.08	11.3	0.009
5-11-94	1001	0.51	11.1	-0.45	10.5	0.56	6.0	-0.07	10.5	0.016
5-12-94	0939	0.58	11.1	0.43	5.3	0.58	5.1	0.25	5.3	0.011
5-13-96	1316	0.42	8.9	-0.42	8.9	0.52	5.7	-0.07	8.9	0.019
5-13-94	1323	0.61	6.1	-0.56	4.7	0.80	4.7	-0.37	4.7	0.040
5-17-94	1327	0.48	8.1	0.34	7.2	-0.60	6.0	0.11	7.2	-0.018

* Times are approximate.

† "low" indicates that the absolute value is less than 0.001 in.

Table A-4: The Arvida House

Radial Direction (Parallel to Major Roof Line)										
Shot Date	Time *	Maximum Ground Vibration, $V_G(t_1)$ in/s	Frequency, Hz	Driving Ground Vibration, $V_G(t_2)$ in/s	Frequency, Hz	Maximum High Corner Structure Response, $V_{High}(t_3)$ in/s	Frequency, Hz	Corresponding Low Corner Structure Response, $V_{Low}(t_3)$ in/s	Frequency, Hz	Maximum High-Low Differential Displacement, in
4-6-95	1111	0.44	20.4	0.21	25.6	0.28	11.3	0.19	25.6	0.003
4-6-95	1126	0.10	64.0	0.07	5.3	0.12	9.6	0.07	5.3	low
4-6-95†	1126	0.07	9.4	0.05	8.8	-0.04	9.5	-0.01	9.0	-0.001
4-6-95	1159	-0.16	39.3	0.13	7.8	0.19	7.3	0.13	7.8	0.001
4-6-95‡	1159	0.14	5.7	0.13	7.8	0.19	7.3	0.13	7.8	0.001

Vertical Direction										
Shot Date	Time *	Maximum Ground Vibration, $V_G(t_1)$ in/s	Frequency, Hz	Driving Ground Vibration, $V_G(t_2)$ in/s	Frequency, Hz	Maximum High Corner Structure Response, $V_{High}(t_3)$ in/s	Frequency, Hz	Corresponding Low Corner Structure Response, $V_{Low}(t_3)$ in/s	Frequency, Hz	Maximum High-Low Differential Displacement, in†
4-6-95	1111	0.33	64.0	0.22	46.3	0.27	23.2	0.22	46.3	0.001
4-6-95	1126	-0.12	64.0	-0.15	7.1	0.15	7.5	0.14	7.1	low (0.000)
4-6-95‡	1126	0.15	7.0	0.15	7.1	0.15	7.2	0.15	6.3	0.004
4-6-95	1159	0.21	56.8	-0.17	8.0	-0.17	8.4	-0.17	8.0	low
4-6-95‡	1159	-0.19	7.9	-0.17	8.0	-0.17	8.4	-0.17	8.0	low

Transverse Direction (Perpendicular to Major Roof Line)										
Shot Date	Time *	Maximum Ground Vibration, $V_G(t_1)$ in/s	Frequency, Hz	Driving Ground Vibration, $V_G(t_2)$ in/s	Frequency, Hz	Maximum High Corner Structure Response, $V_{High}(t_3)$ in/s	Frequency, Hz	Corresponding Low Corner Structure Response, $V_{Low}(t_3)$ in/s	Frequency, Hz	Maximum High-Low Differential Displacement, in
4-6-95#	1111	-0.26	42.6	0.15	8.8	0.69	10.2	0.10	8.8	0.009

* Times are approximate.

† "low" indicates that the absolute value is less than 0.001 in.

‡ Measurements from the low frequency portion of the same event listed on the line above.

Only this event produced high enough amplitude transverse component for a reliable differential displacement measurement to be made.

Table A-5: The Jordan House

Radial Direction (Parallel to Major Roof Line)							
Shot Date	Time *	Maximum Ground Vibration, $ V_G(t_1) $ in/s	Frequency, Hz	Driving Ground Vibration, $ V_G(t_2) $ in/s	Frequency, Hz	Maximum High Corner Structure Response, $ V_{High}(t_3) $ in/s	Frequency, Hz
6-10-93	1537	0.18	32.0	0.12	5.7	0.24	9.8
6-11-93	1601	0.23	30.0	0.20	6.0	0.31	6.0

Vertical Direction							
Shot Date	Time *	Maximum Ground Vibration, $ V_G(t_1) $ in/s	Frequency, Hz	Driving Ground Vibration, $ V_G(t_2) $ in/s	Frequency, Hz	Maximum High Corner Structure Response, $ V_{High}(t_3) $ in/s	Frequency, Hz
6-10-93	1537	0.35	75	0.35	75	0.21	50
6-11-93	1601	0.38	59	0.38	59	0.27	59

Transverse Direction (Perpendicular to Major Roof Line)							
Shot Date	Time *	Maximum Ground Vibration, $ V_G(t_1) $ in/s	Frequency, Hz	Driving Ground Vibration, $ V_G(t_2) $ in/s	Frequency, Hz	Maximum High Corner Structure Response, $ V_{High}(t_3) $ in/s	Frequency, Hz
6-10-93	1537	0.17	19	0.08	2.6	0.03	4.9
6-11-93	1601	0.32	2.5	0.32	2.5	0.05	3.4

* Times are approximate.

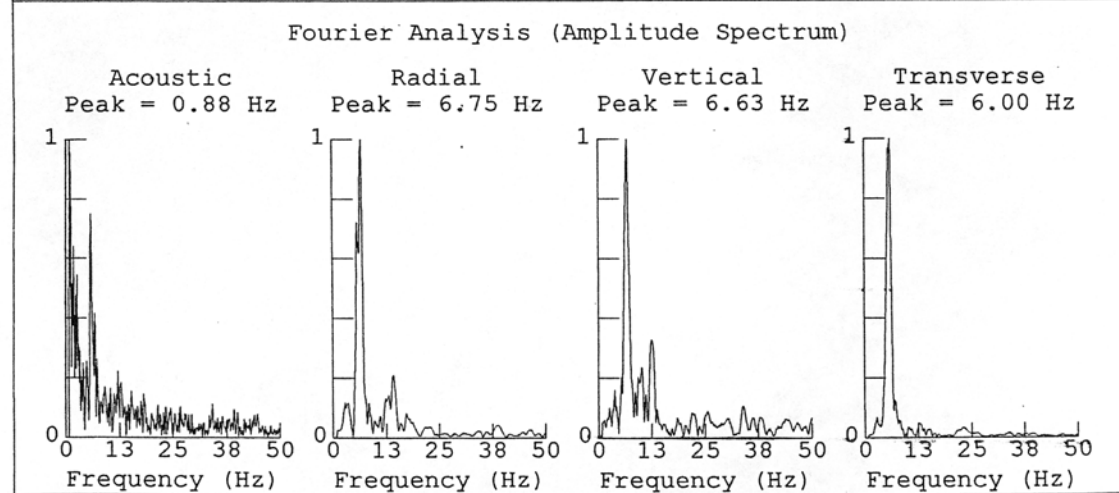
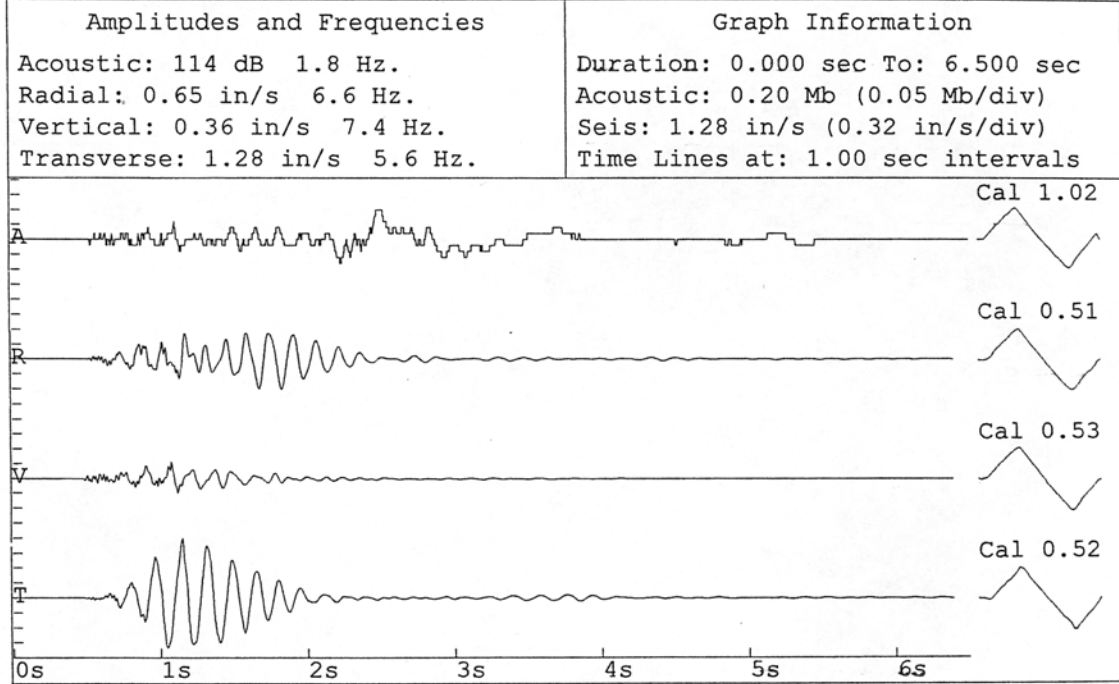
APPENDIX B: SELECTED GROUND VIBRATION AND STRUCTURE RESPONSE RECORDINGS

The following ground vibration and structure response recordings are matched according to location and date and are time synchronized.

Important: Because of the recording setup used, the individual components of motion for ground vibration and structure response may not be the same for a particular event. For example, the transverse direction on the ground vibration for an event may correspond to the vertical direction on the structure response record. Refer to the directional key in the header of each vibration record for proper orientation between individual ground vibration and structure response components of motion. Also note that in comparing ground vibration and structure response recordings, east velocity amplitude = minus west velocity amplitude and north velocity amplitude = minus south amplitude (i.e., north velocity amplitude = $-1 \times$ south velocity amplitude).

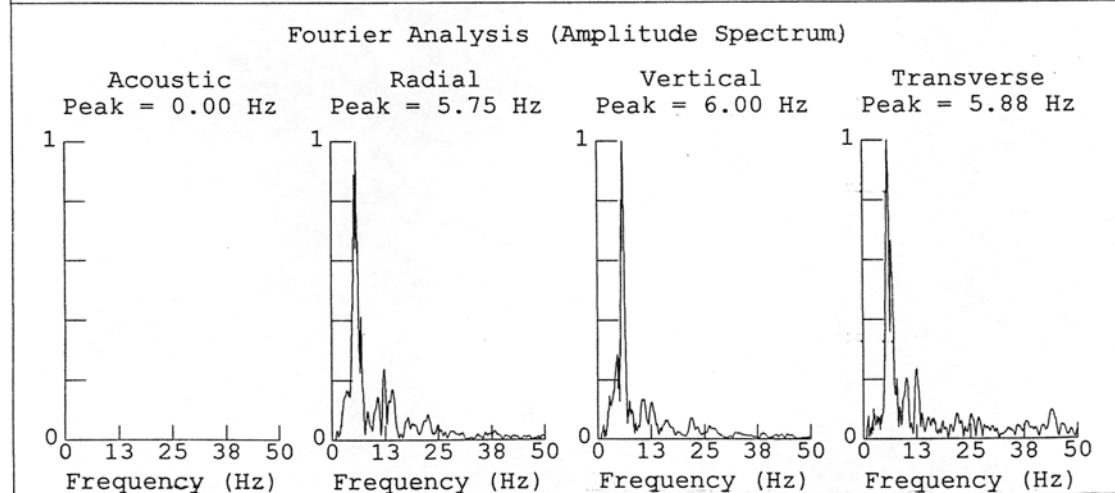
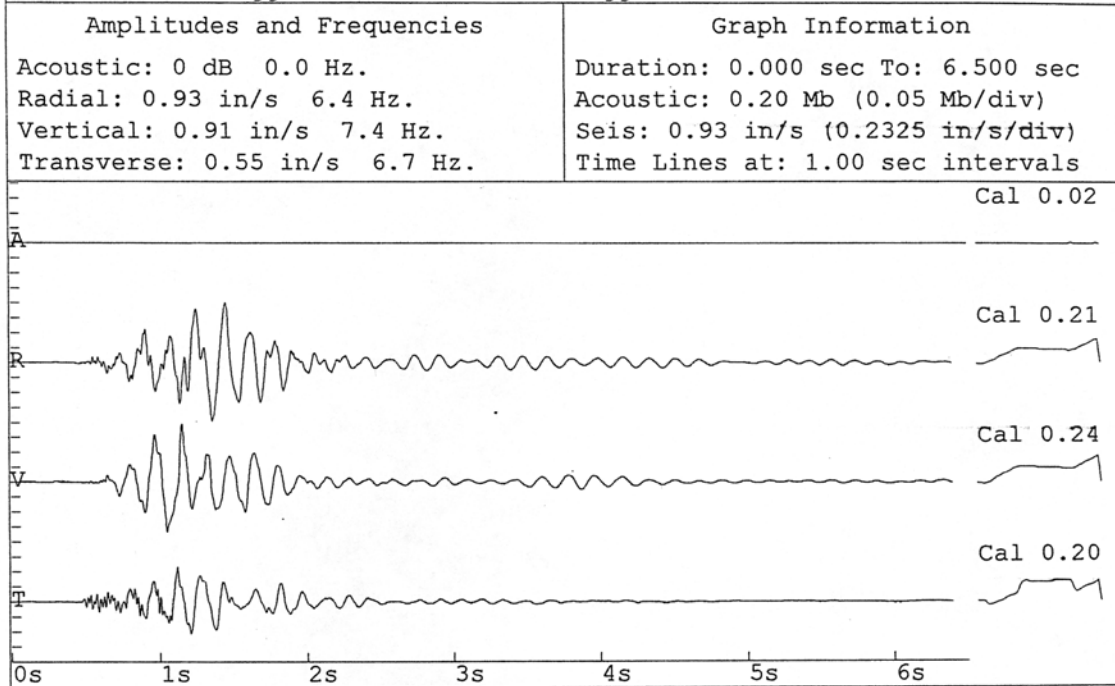
The Shack, Amax Minnehaha Mine
Ground Vibration, NE corner
R = east, V = up, T = south

Event: 002 Date: 10/12/93 Time: 12:36
Air Trigger: 142 dB Seis Trigger: 0.05 in/s S/N: 85



The Shack, Amax Minnehaha Mine
 Structure Response, NE corner (low)
 R = east, V = south, T = down

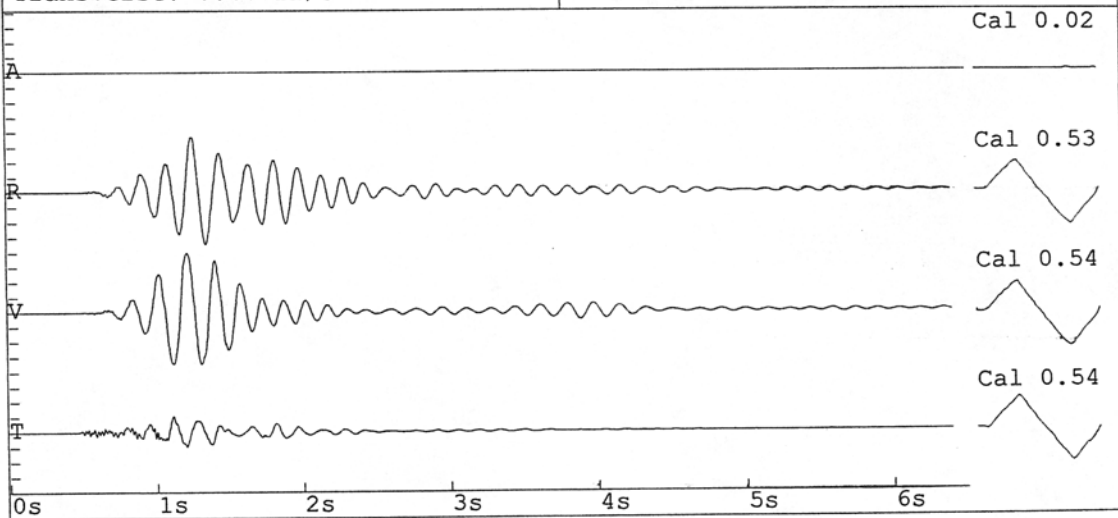
Event: 002 Date: 10/12/93 Time: 12:34
 Air Trigger: 142 dB Seis Trigger: 0.05 in/s S/N: 87



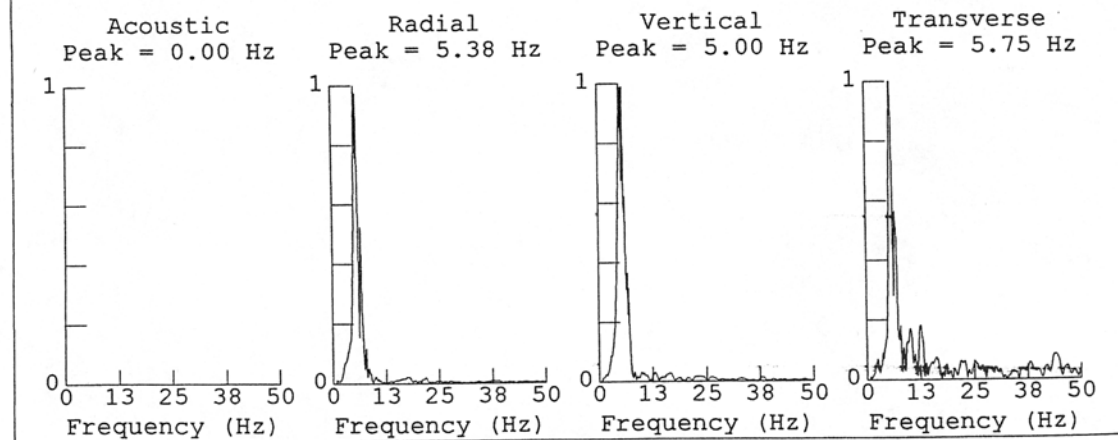
The Shack, Amax Minnehaha Mine
 Structure Response, NE corner (high)
 R = east, V = south, T = down

Event: 002 Date: 10/12/93 Time: 12:34
 Air Trigger: 142 dB Seis Trigger: 0.05 in/s S/N: 86

Amplitudes and Frequencies	Graph Information
Acoustic: 0 dB 0.0 Hz.	Duration: 0.000 sec To: 6.500 sec
Radial: 2.08 in/s 5.3 Hz.	Acoustic: 0.20 Mb (0.05 Mb/div)
Vertical: 2.24 in/s 5.0 Hz.	Seis: 2.24 in/s (0.56 in/s/div)
Transverse: 0.60 in/s 7.1 Hz.	Time Lines at: 1.00 sec intervals

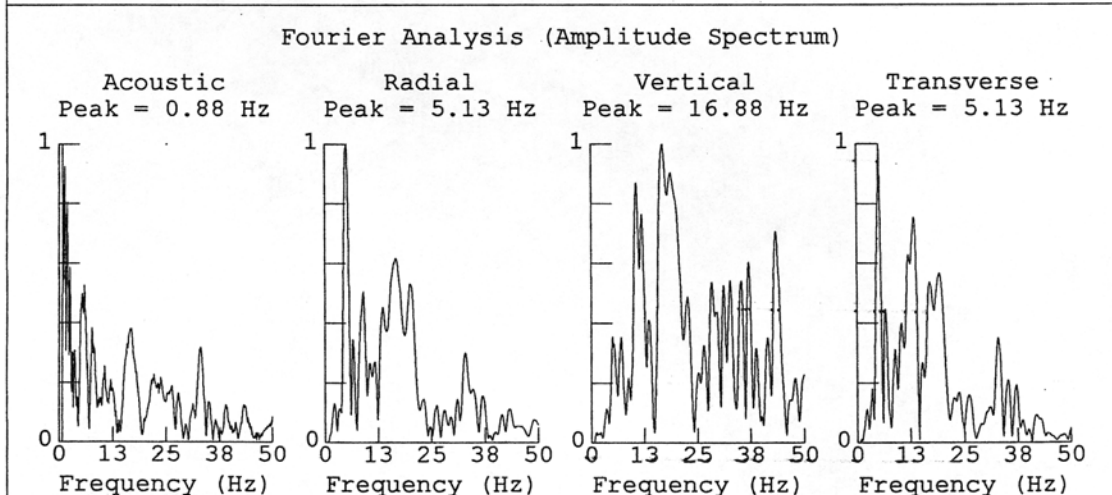
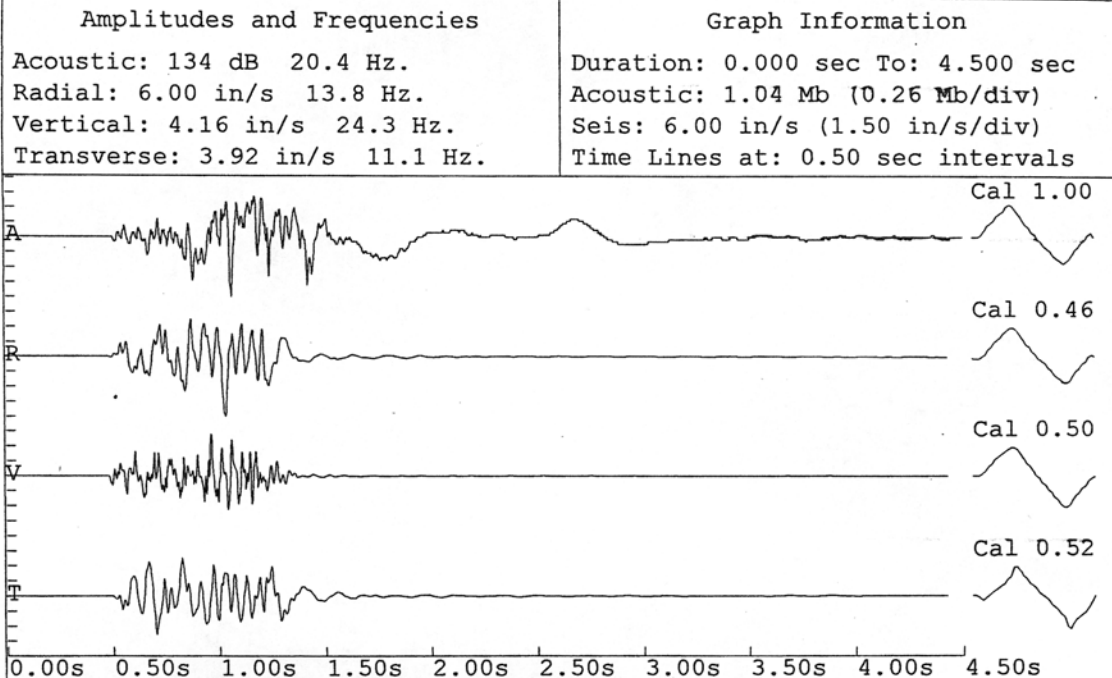


Fourier Analysis (Amplitude Spectrum)



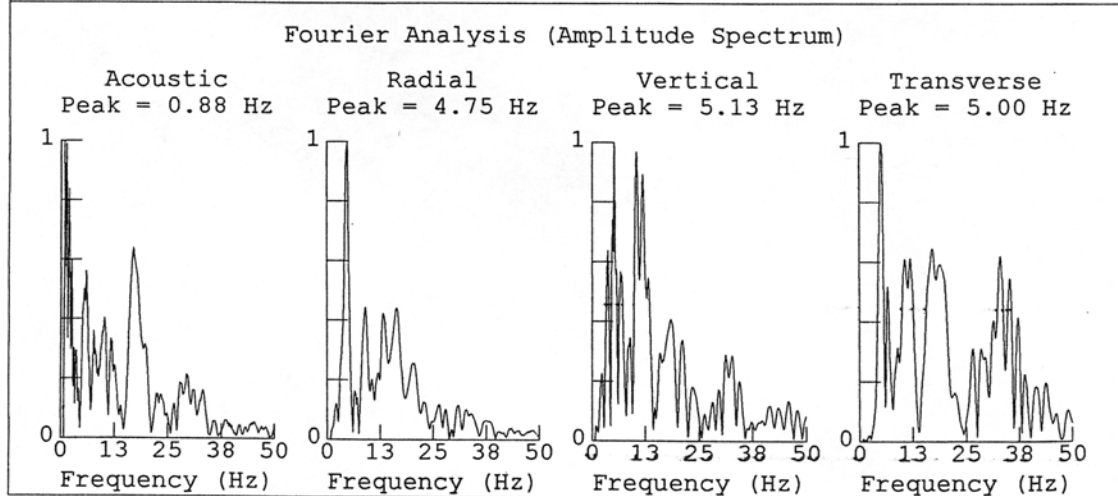
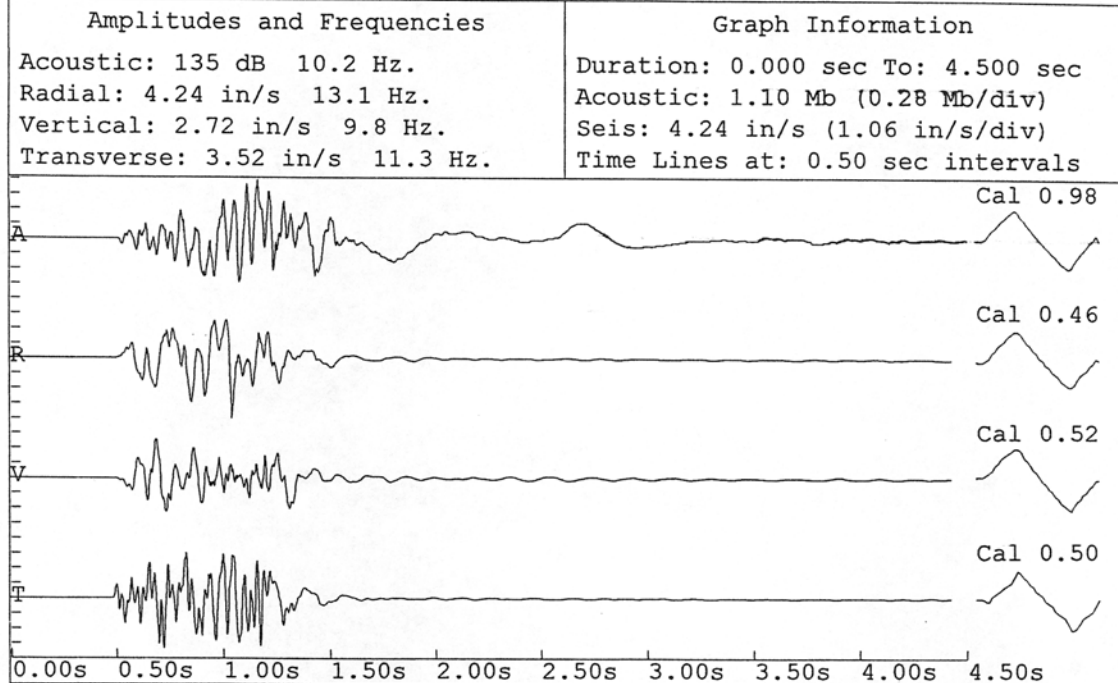
The Shack, Minnehaha Mine
Ground vibration, NE corner
R=east, V=up, T=south

Event: 007 Date: 8/23/94 Time: 17:49
Air Trigger: 148 dB Seis Trigger: 0.26 in/s S/N: 85



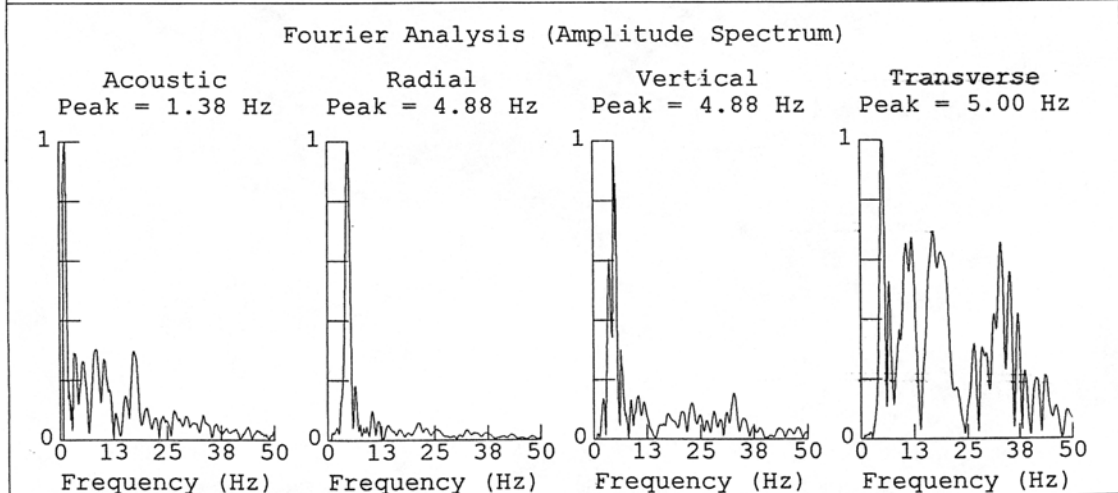
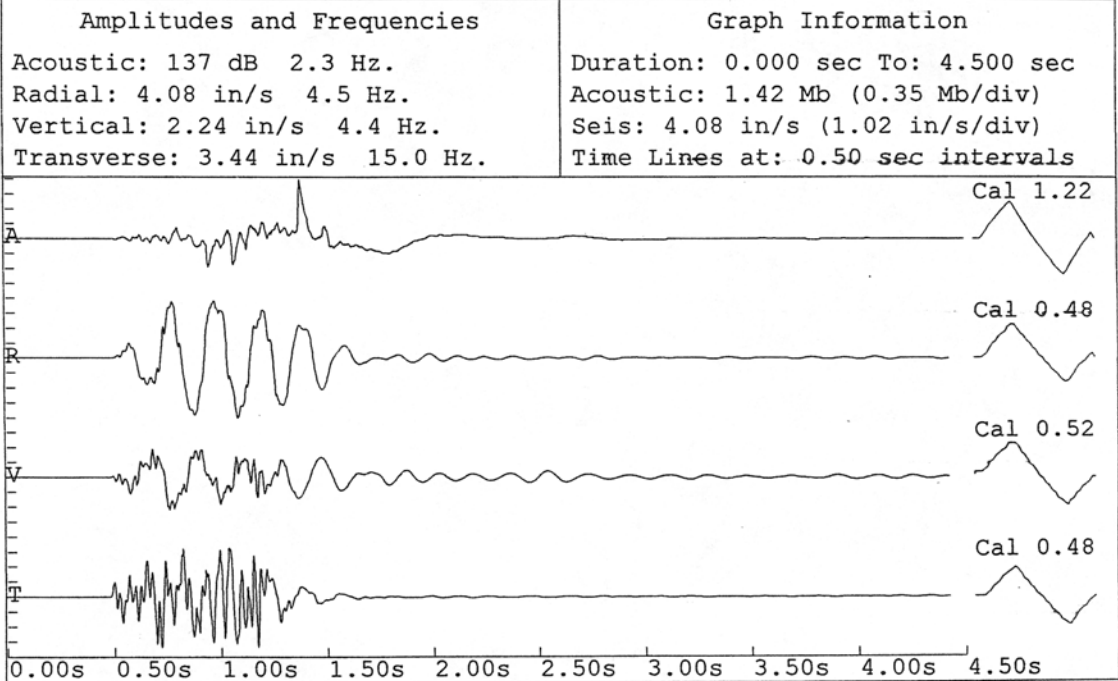
The Shack, Minnehaha Mine
 Structure response, NE corner(low)
 R=east, V=south, T=down

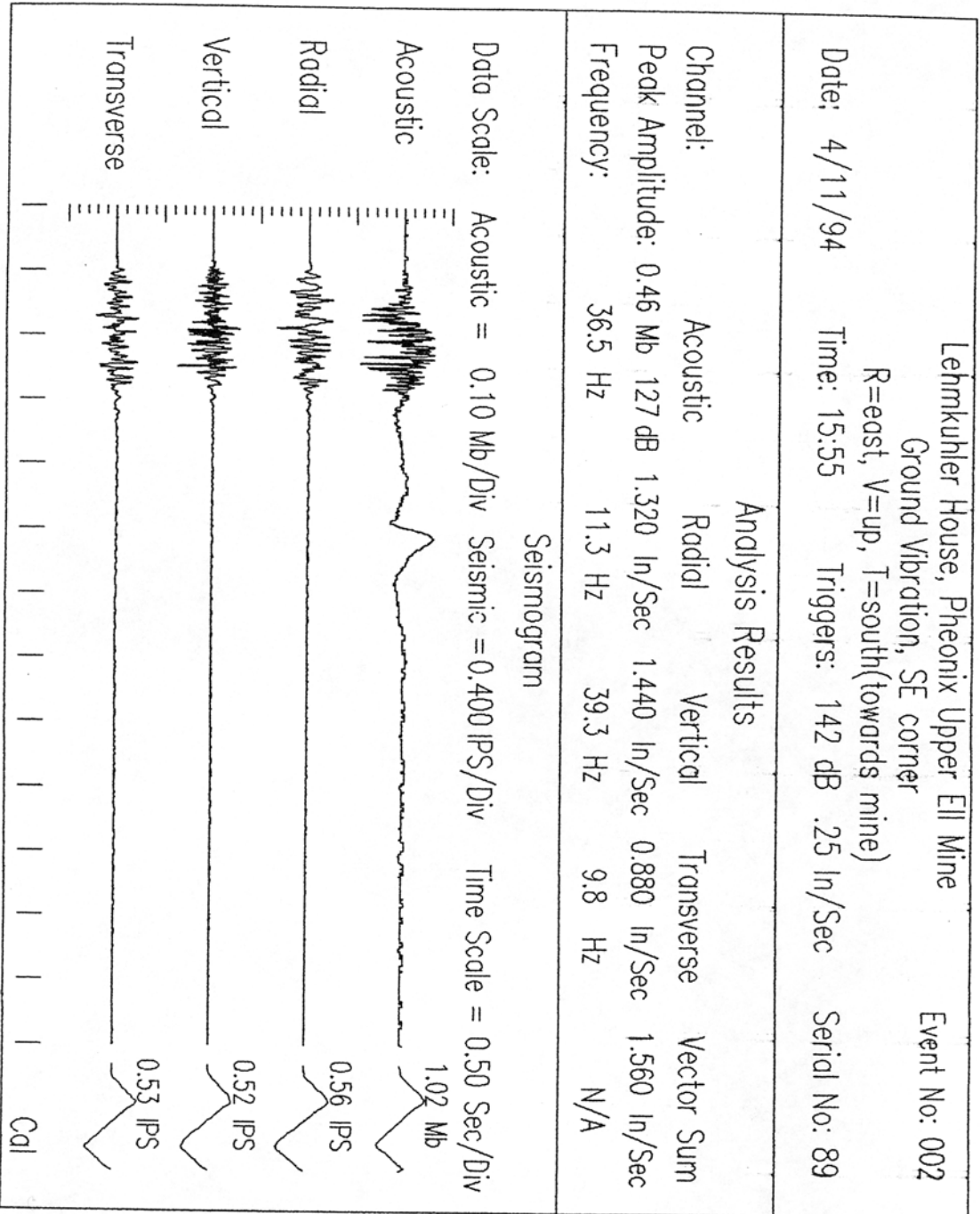
Event: 007 Date: 8/23/94 Time: 17:48
 Air Trigger: 142 dB Seis Trigger: 2.28 in/s S/N: 87

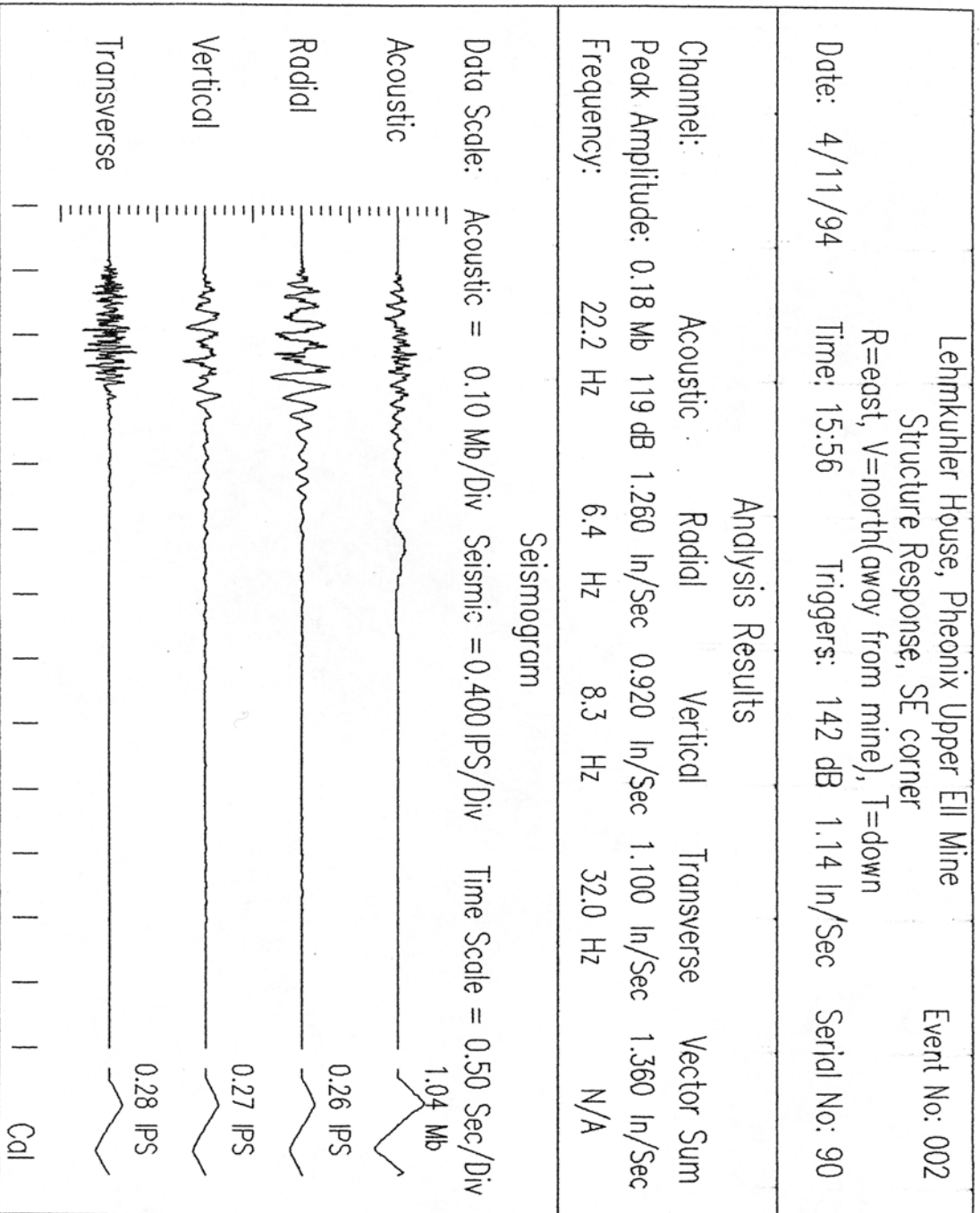


The Shack, Minnehaha Mine
 Structure response, NE corner (high)
 R=east, V=south, T=down

Event: 007 Date: 8/23/94 Time: 17:48
 Air Trigger: 142 dB Seis Trigger: 2.28 in/s S/N: 86







Lehmkuhler House, Pheonix Upper Ell Mine

Lehmkuhler House, Pheonix Upper Ell Mine

Ground Vibration, SE corner

R=east, V=up, T=south (towards mine)

Event: 034 Date: 6/ 9/94 Time: 10:29

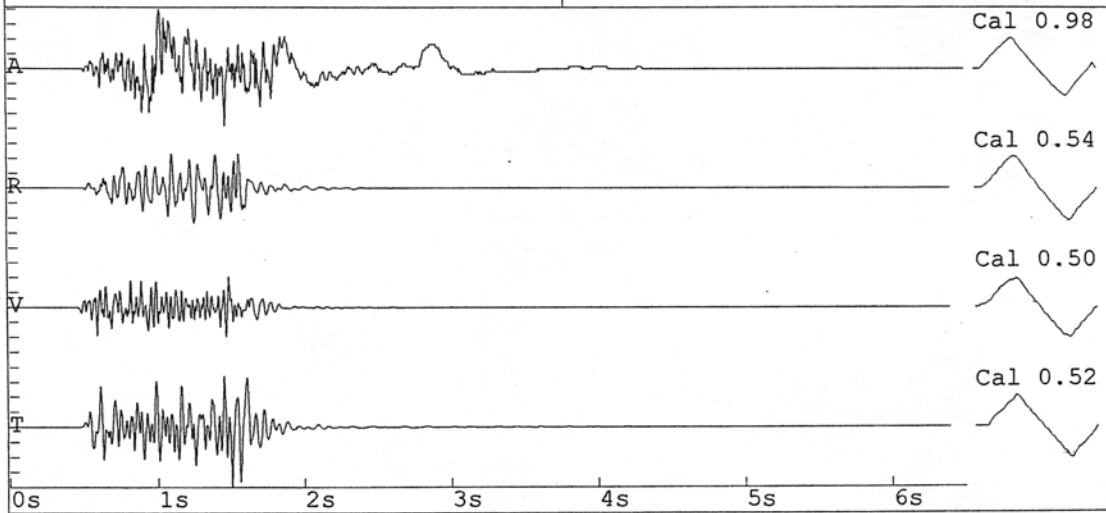
Air Trigger: 142 dB Seis Trigger: 0.25 in/s S/N: 89

Amplitudes and Frequencies

Acoustic: 127 dB 16.0 Hz.
Radial: 1.64 in/s 16.0 Hz.
Vertical: 1.48 in/s 16.0 Hz.
Transverse: 2.80 in/s 18.2 Hz.

Graph Information

Duration: 0.000 sec To: 6.500 sec
Acoustic: 0.44 Mb (0.11 Mb/div)
Seis: 2.80 in/s (0.70 in/s/div)
Time Lines at: 1.00 sec intervals



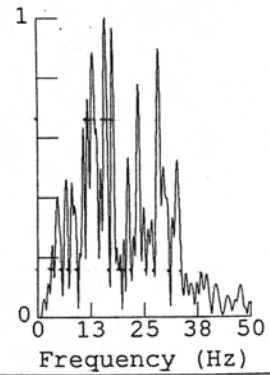
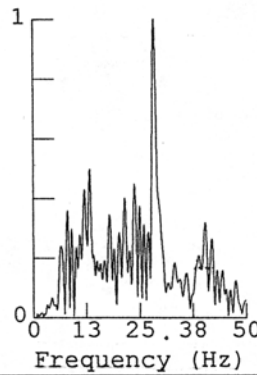
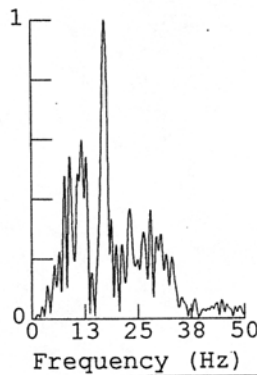
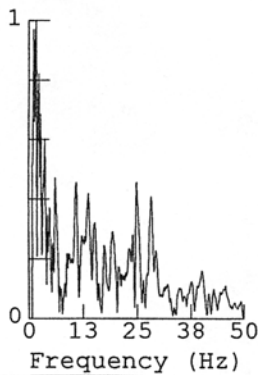
Fourier Analysis (Amplitude Spectrum)

Acoustic
Peak = 1.75 Hz

Radial
Peak = 17.25 Hz

Vertical
Peak = 28.38 Hz

Transverse
Peak = 16.00 Hz



Lehmkuhler House, Peonix UpperEll Mine
 Structure Response, SE corner(low)
 R=east, V=north(away from mine), T=up

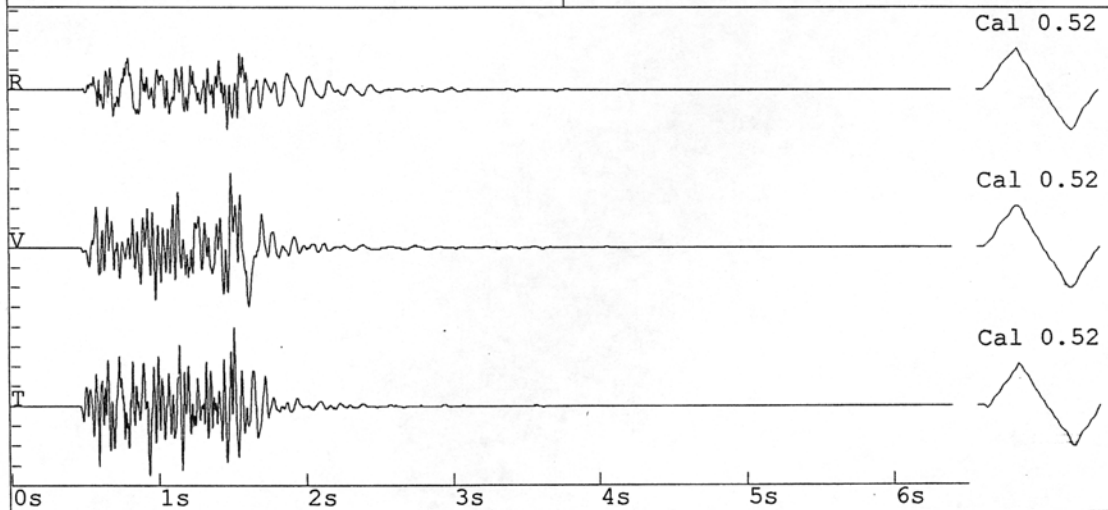
Event: 034 Date: 6/ 9/94 Time: 10:29
 Air Trigger: 142 dB Seis Trigger: 1.14 in/s S/N: 88

Amplitudes and Frequencies

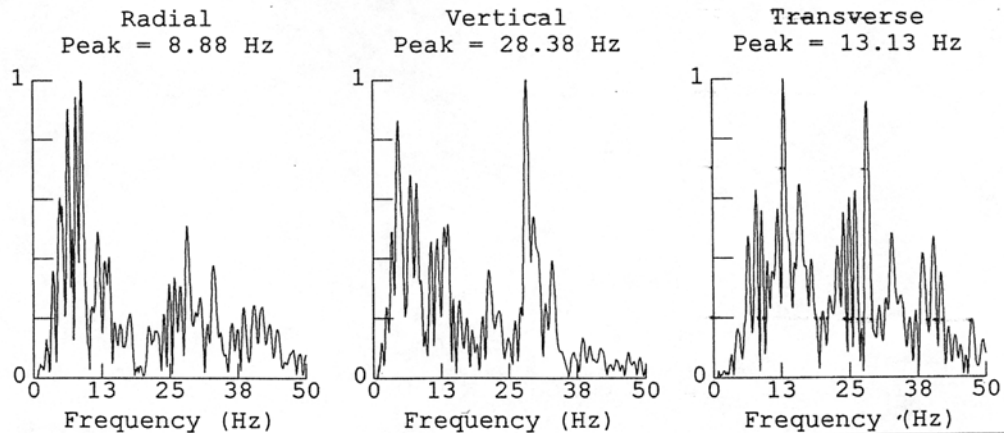
Radial: 0.62 in/s 23.2 Hz.
 Vertical: 1.18 in/s 9.1 Hz.
 Transverse: 1.24 in/s 22.2 Hz.

Graph Information

Duration: 0.000 sec To: 6.500 sec
 Seis: 1.24 in/s (0.31 in/s/div)
 Time Lines at: 1.00 sec intervals



Fourier Analysis (Amplitude Spectrum)



Lehmkuhler House, Pheonix Upper Ell Mine

Lehmkuhler House, Pheonix Upper Ell Mine
Structure Response, SE corner(high)
R=east, V=north(away from mine), T=up

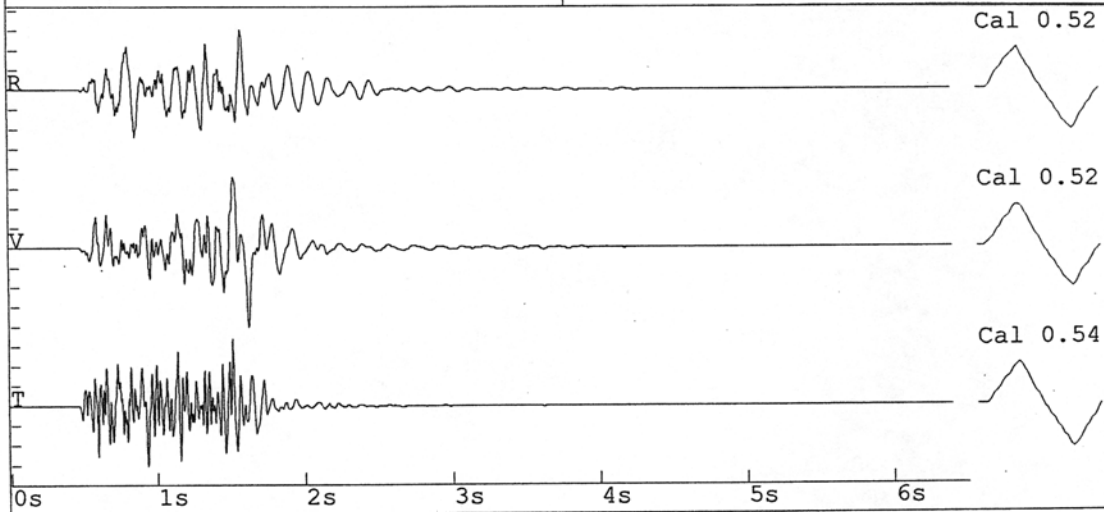
Event: 034 Date: 6/ 9/94 Time: 10:29
Air Trigger: 142 dB Seis Trigger: 1.14 in/s S/N: 90

Amplitudes and Frequencies

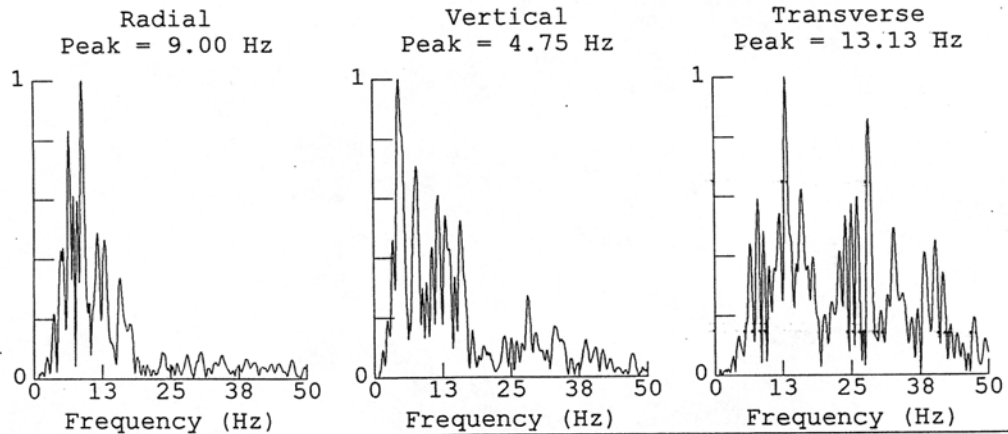
Radial: 1.12 in/s 9.4 Hz.
Vertical: 1.46 in/s 5.6 Hz.
Transverse: 1.24 in/s 23.2 Hz.

Graph Information

Duration: 0.000 sec To: 6.500 sec
Seis: 1.46 in/s (0.365 in/s/div)
Time Lines at: 1.00 sec intervals



Fourier Analysis (Amplitude Spectrum)



Lehmkuhler House, Pheonix Upper Ell Mine

Lhemkuhler House, Upper Ell Mine
Ground Vibration, SE corner
R=east, V=up, T=south (towards mine)

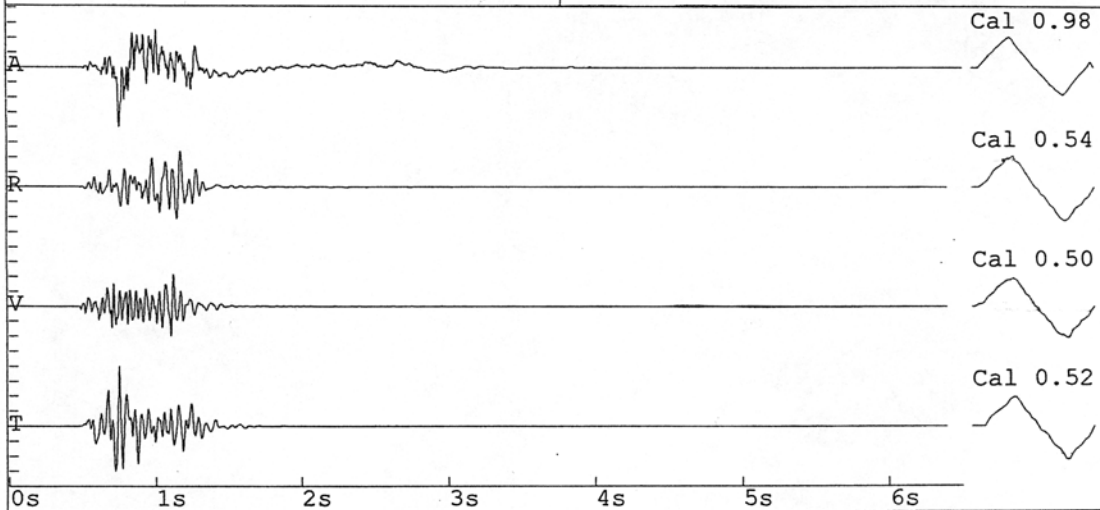
Event: 013 Date: 5/27/94 Time: 15:31
Air Trigger: 142 dB Seis Trigger: 0.25 in/s S/N: 89

Amplitudes and Frequencies

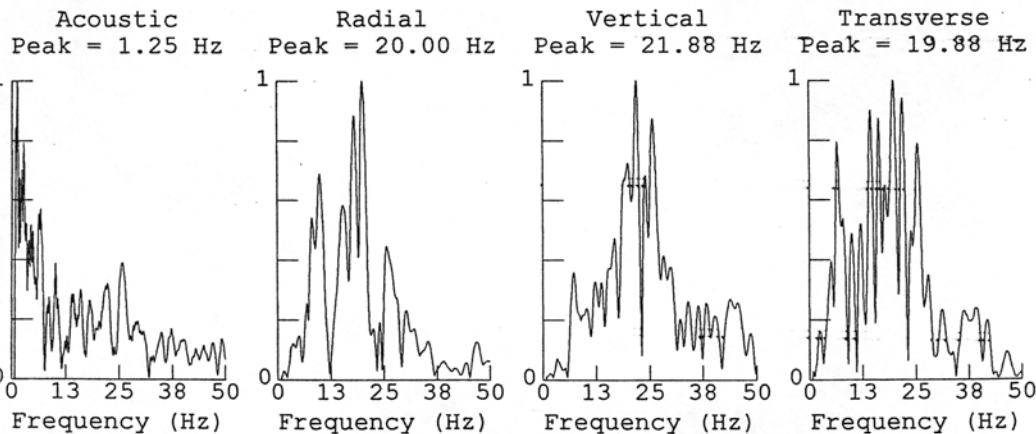
Acoustic: 135 dB 9.8 Hz.
Radial: 2.96 in/s 16.0 Hz.
Vertical: 2.64 in/s 23.2 Hz.
Transverse: 4.96 in/s 21.3 Hz.

Graph Information

Duration: 0.000 sec To: 6.500 sec
Acoustic: 1.10 Mb (0.28 Mb/div)
Seis: 4.96 in/s (1.24 in/s/div)
Time Lines at: 1.00 sec intervals



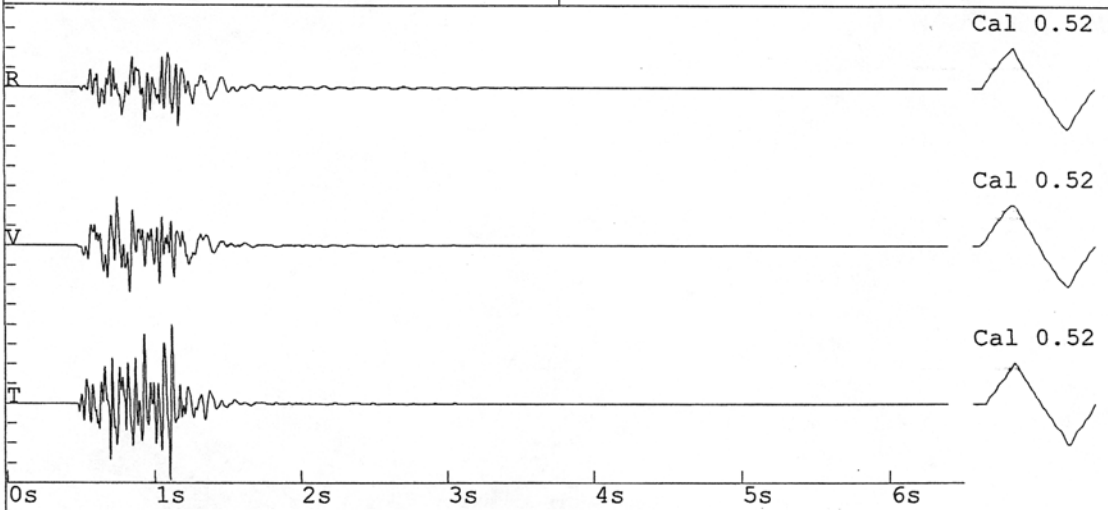
Fourier Analysis (Amplitude Spectrum)



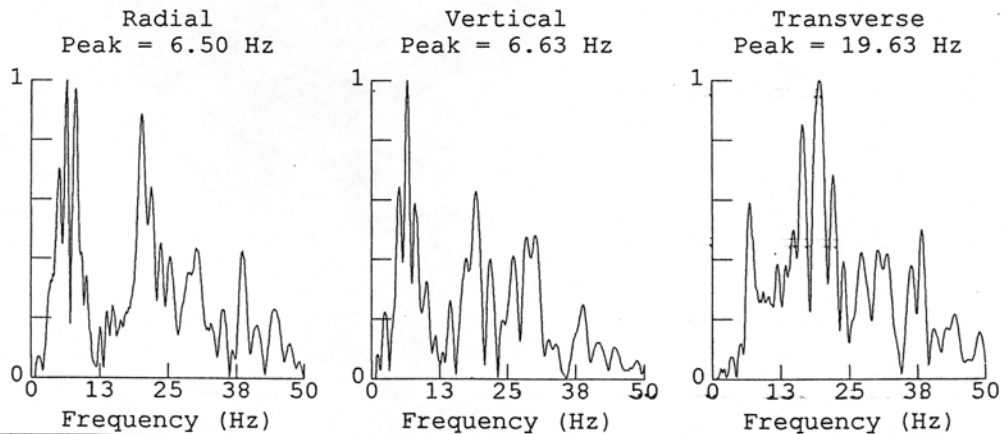
Lhemkuhler House, Upper Ell Mine
 Structure Response, SE corner(low)
 R=east, V=north(away from mine), T=up

Event: 013 Date: 5/27/94 Time: 15:31
 Air Trigger: 142 dB Seis Trigger: 1.14 in/s S/N: 88

Amplitudes and Frequencies	Graph Information
Radial: 1.14 in/s 26.9 Hz. Vertical: 1.42 in/s 16.0 Hz. Transverse: 2.32 in/s 24.3 Hz.	Duration: 0.000 sec To: 6.500 sec Seis: 2.32 in/s (0.58 in/s/div) Time Lines at: 1.00 sec intervals



Fourier Analysis (Amplitude Spectrum)



Lehmkuhler House, Pheonix Upper Ell Mine

Lhemkuhler House, Upper Ell Mine

Structure Response, SE corner(^{high})

R=east, V=north(away from mine), T=up

Event: 013 Date: 5/27/94 Time: 15:31

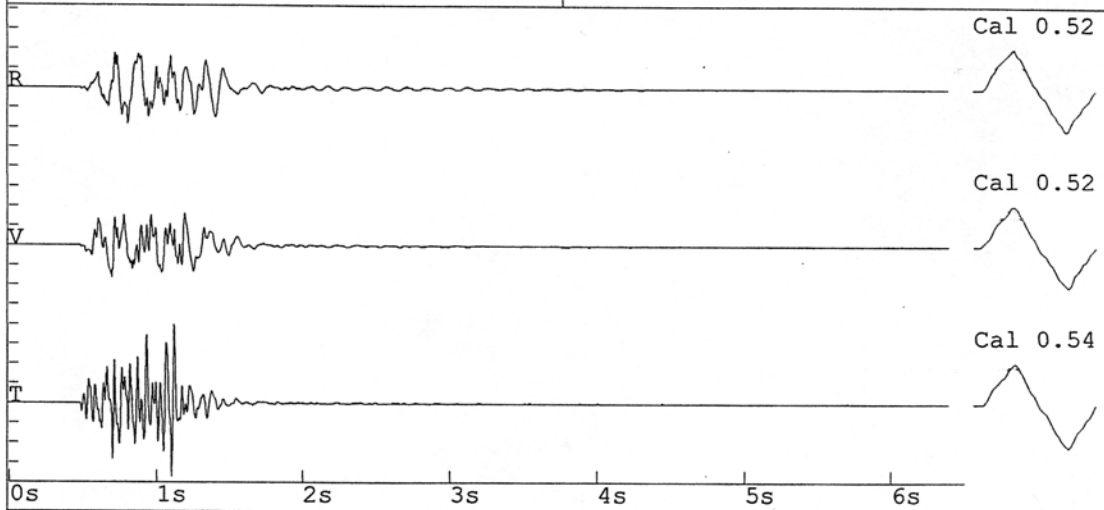
Air Trigger: 142 dB Seis Trigger: 1.14 in/s S/N: 90

Amplitudes and Frequencies

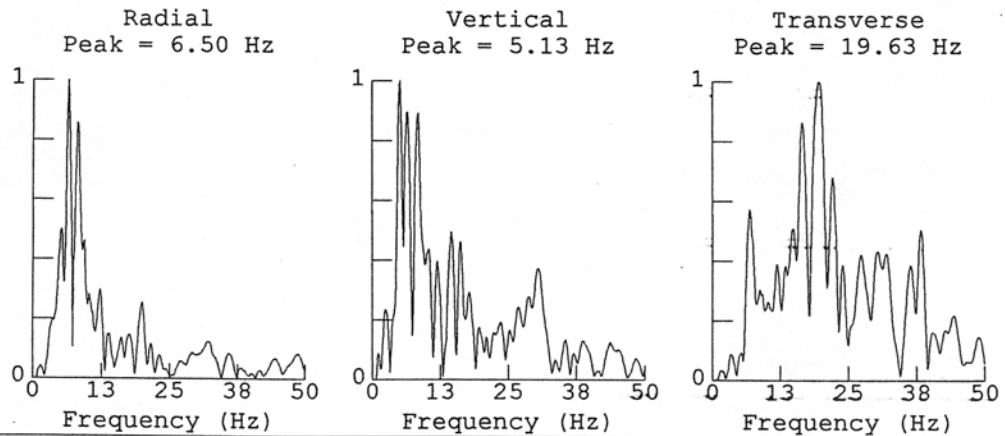
Radial: 1.10 in/s 5.8 Hz.
Vertical: 0.98 in/s 12.4 Hz.
Transverse: 2.40 in/s 23.2 Hz.

Graph Information

Duration: 0.000 sec To: 6.500 sec
Seis: 2.40 in/s (0.60 in/s/div)
Time Lines at: 1.00 sec intervals

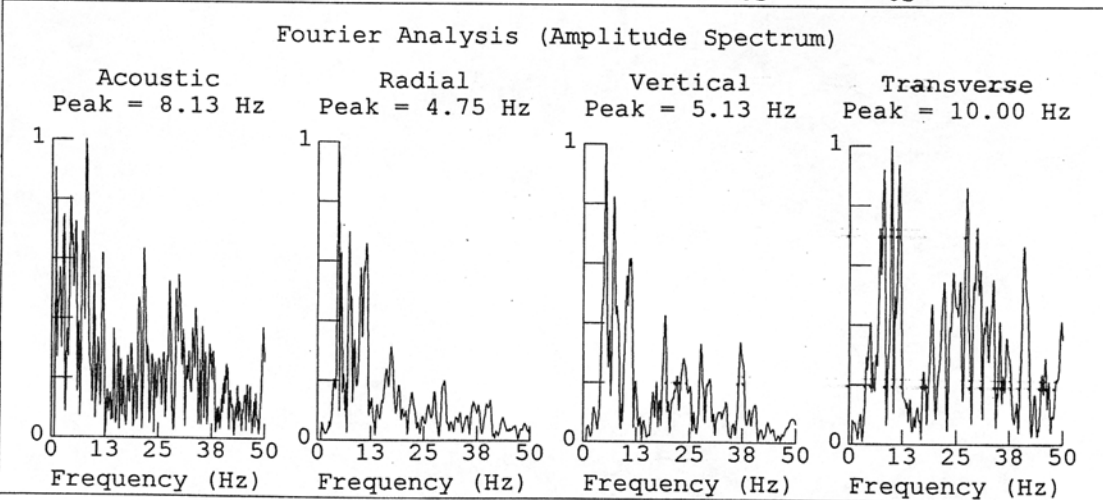
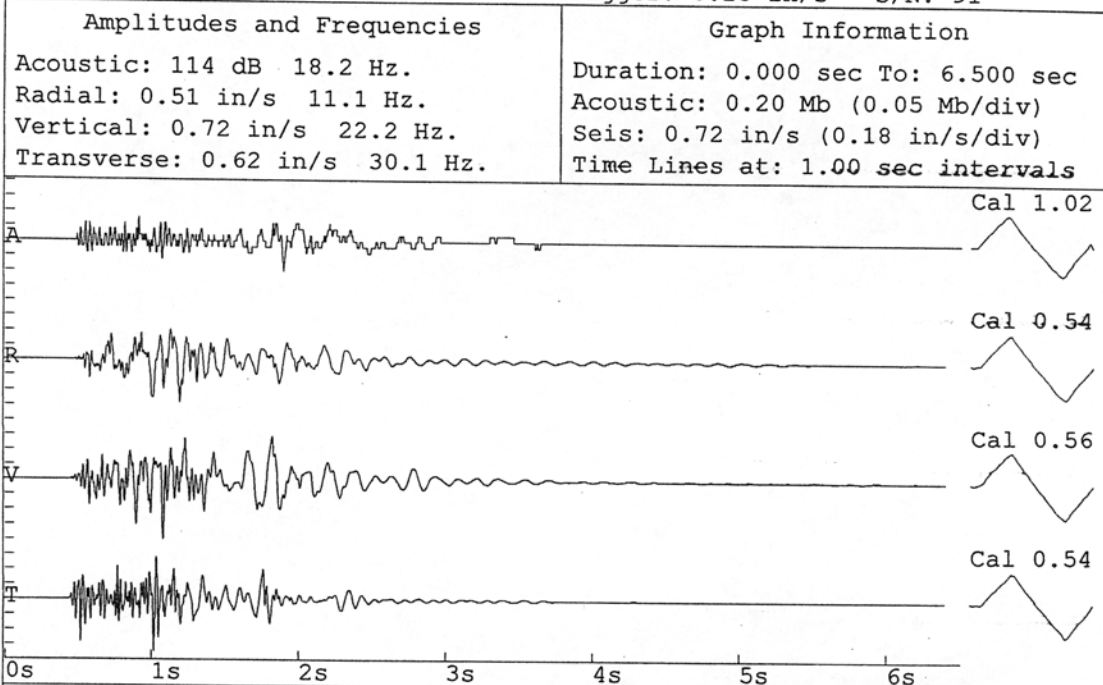


Fourier Analysis (Amplitude Spectrum)



Smith House, AMAX Chinook Mine
Ground Vibration/Low Corner, NW corner
R=west, V=north, T=down

Event: 018 Date: 5/12/94 Time: 9:39
Air Trigger: 142 dB Seis Trigger: 0.25 in/s S/N: 91



Smith House, AMAX Chinook Mine
 Structure response, NW corner (high)
 R=west, V=south, T=up

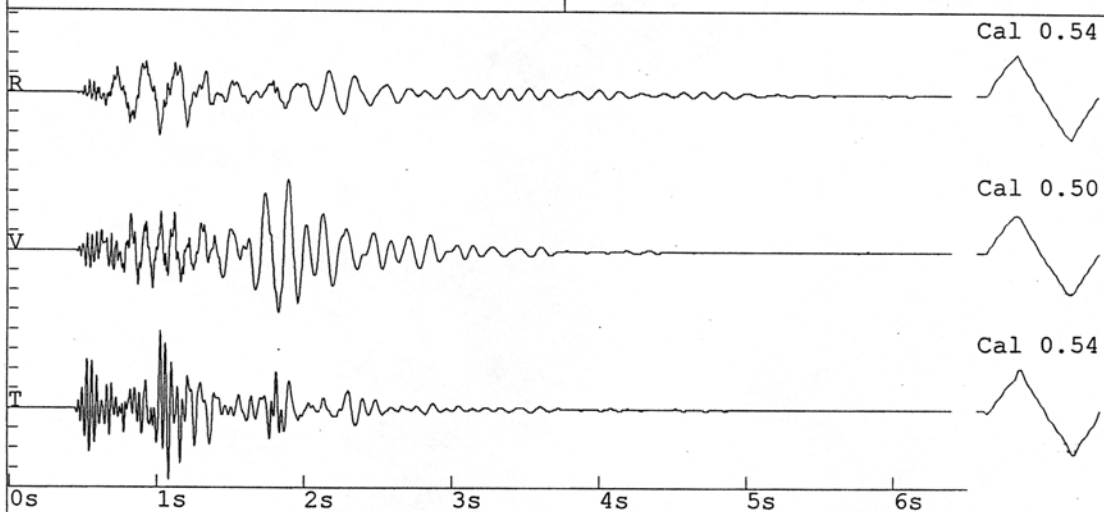
Event: 019 Date: 5/12/94 Time: 9:44
 Air Trigger: 142 dB Seis Trigger: 1.00 in/s S/N: 92

Amplitudes and Frequencies

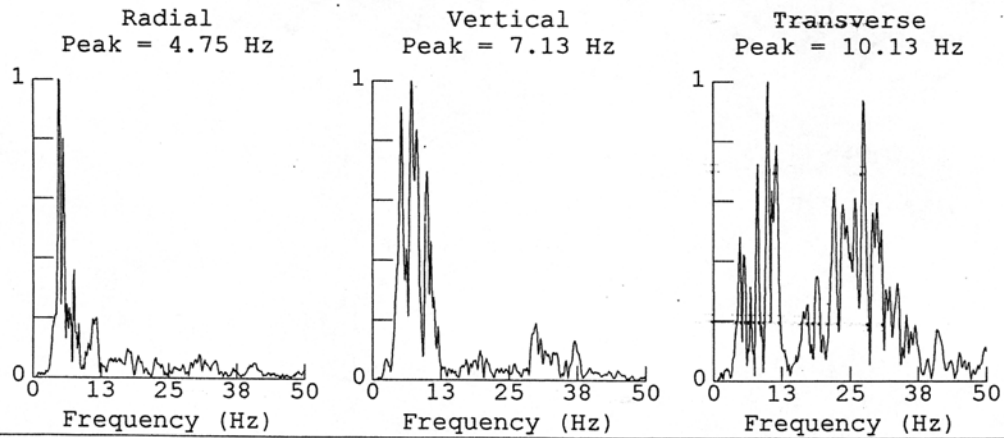
Radial: 0.56 in/s 6.0 Hz.
 Vertical: 0.94 in/s 7.4 Hz.
 Transverse: 1.04 in/s 21.3 Hz.

Graph Information

Duration: 0.000 sec To: 6.500 sec
 Seis: 1.04 in/s (0.26 in/s/div)
 Time Lines at: 1.00 sec intervals



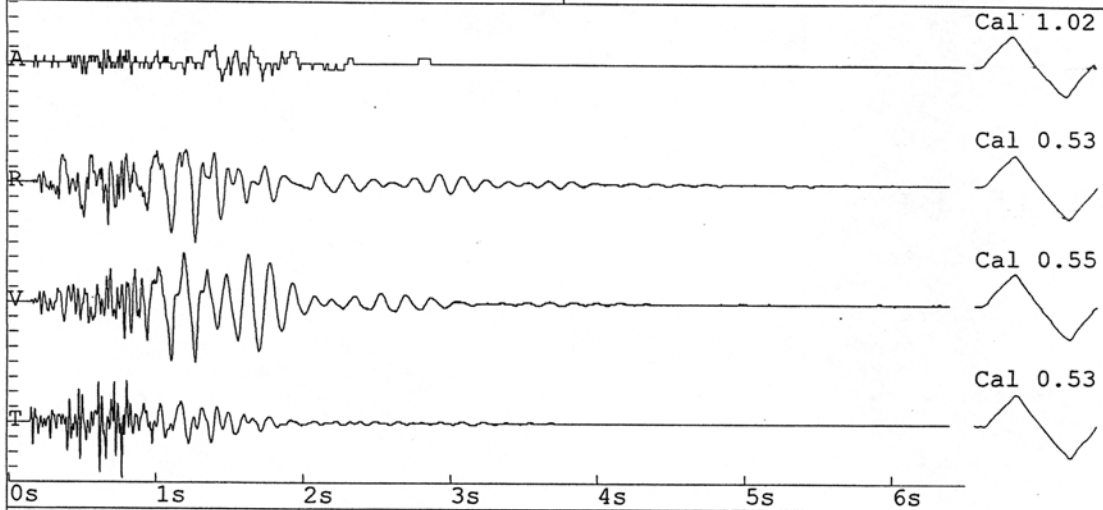
Fourier Analysis (Amplitude Spectrum)



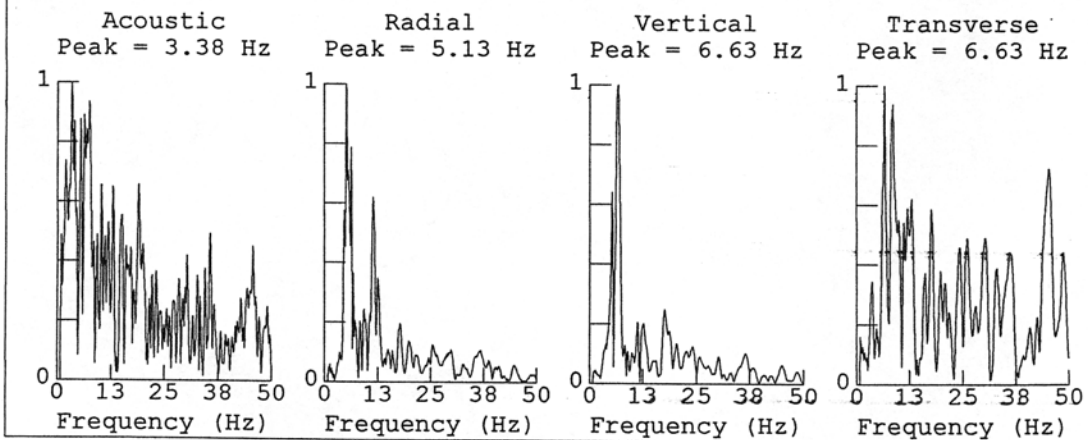
Smith House, AMAX Chinook Mine
Ground Vibration/Low Corner, NE Corner
R=north, V=east(towards mine), T=down

Event: 026 Date: 5/13/94 Time: 13:23
Air Trigger: 142 dB Seis Trigger: 0.25 in/s S/N: 91

Amplitudes and Frequencies	Graph Information
Acoustic: 110 dB 0.0 Hz.	Duration: 0.000 sec To: 6.500 sec
Radial: 0.42 in/s 8.9 Hz.	Acoustic: 0.20 Mb (0.05 Mb/div)
Vertical: 0.42 in/s 8.1 Hz.	Seis: 0.42 in/s (0.105 in/s/div)
Transverse: 0.40 in/s 32.0 Hz.	Time Lines at: 1.00 sec intervals



Fourier Analysis (Amplitude Spectrum)



Smith House, AMAX Chinook Mine
 Structure Response, NE corner high
 R=north, V=west (away from mine), T=up

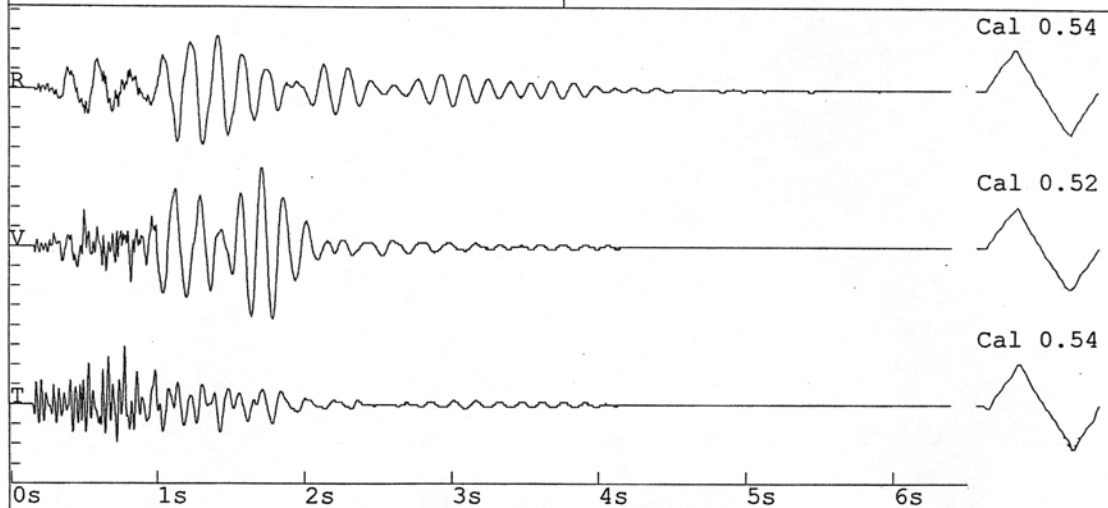
Event: 026 Date: 5/13/94 Time: 13:22
 Air Trigger: 142 dB Seis Trigger: 1.14 in/s S/N: 92

Amplitudes and Frequencies

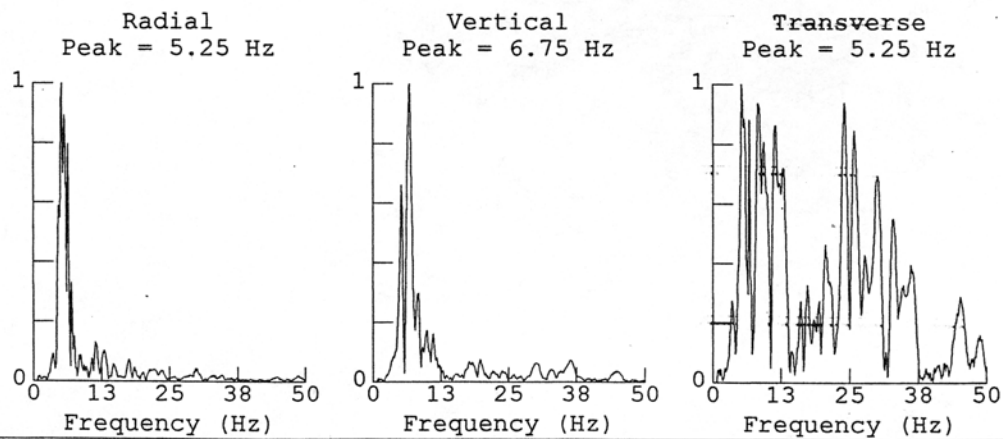
Radial: 0.52 in/s 5.7 Hz.
 Vertical: 0.74 in/s 6.7 Hz.
 Transverse: 0.54 in/s 21.3 Hz.

Graph Information

Duration: 0.000 sec To: 6.500 sec
 Seis: 0.74 in/s (0.185 in/s/div)
 Time Lines at: 1.00 sec intervals



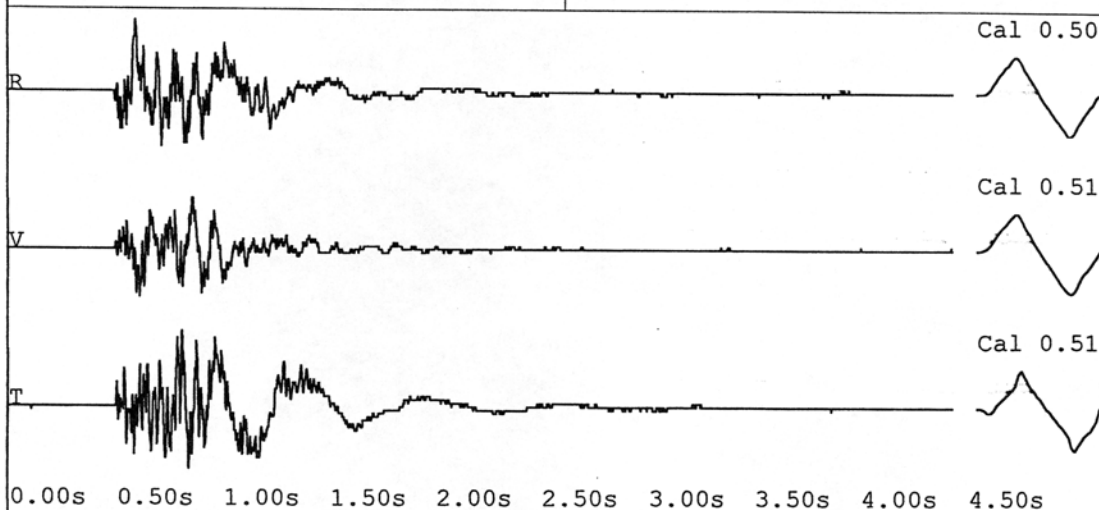
Fourier Analysis (Amplitude Spectrum)



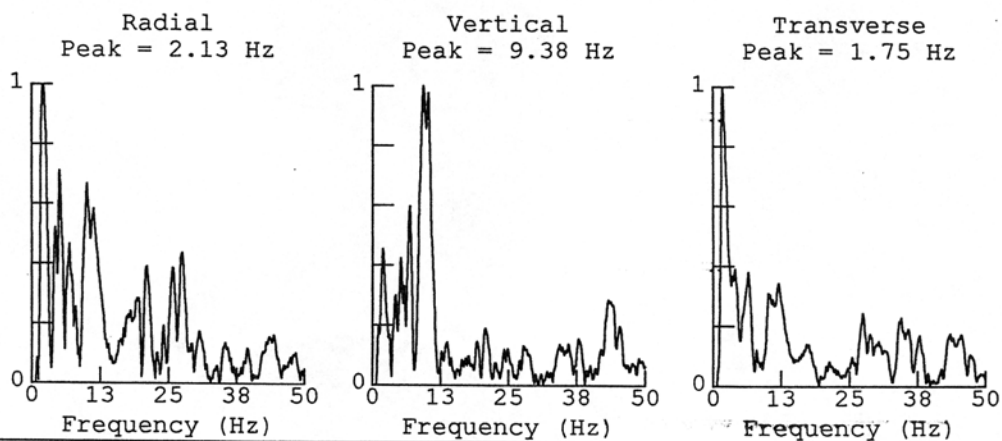
Arvida, Model Home
 Ground Vibration/Low Corner, NE Corner
 R = east, V = south, T = down

Event: 008 Date: 4/ 6/95 Time: 11:11
 Air Trigger: 142 dB Seis Trigger: 1.14 in/s S/N: 88

Amplitudes and Frequencies	Graph Information
Radial: 0.21 in/s 11.6 Hz.	Duration: 0.000 sec To: 4.500 sec
Vertical: 0.15 in/s 11.9 Hz.	Seis: 0.23 in/s (0.0575 in/s/div)
Transverse: 0.23 in/s 23.2 Hz.	Time Lines at: 0.50 sec intervals



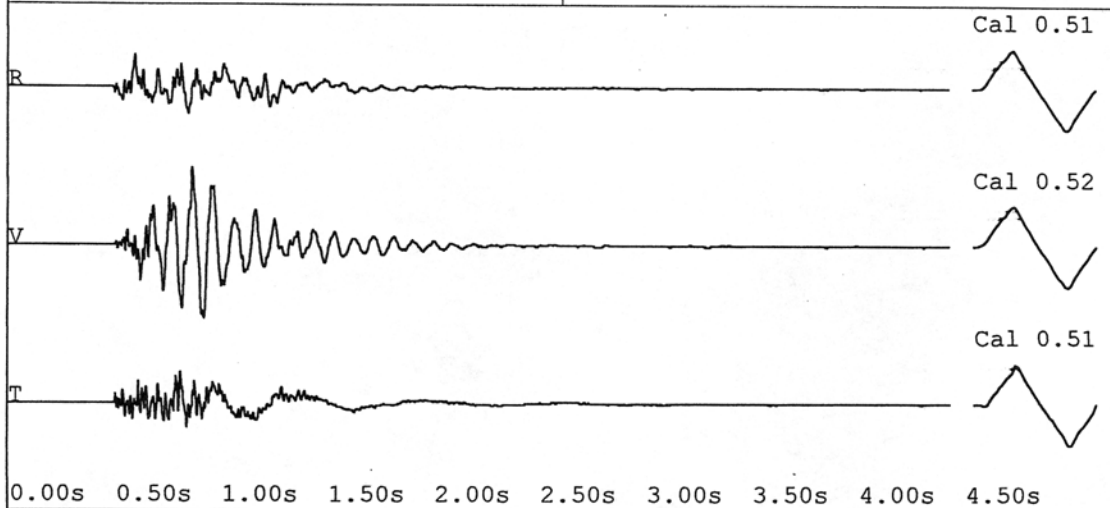
Fourier Analysis (Amplitude Spectrum)



Arvida, Model Home
 Structure Response, NE corner (high)
 R = east, V = south, T = down

Event: 008 Date: 4/ 6/95 Time: 11:11
 Air Trigger: 148 dB Seis Trigger: 1.14 in/s S/N: 85

Amplitudes and Frequencies	Graph Information
Radial: 0.28 in/s 11.3 Hz. Vertical: 0.69 in/s 10.2 Hz. Transverse: 0.27 in/s 23.2 Hz.	Duration: 0.000 sec To: 4.500 sec Seis: 0.69 in/s (0.1725 in/s/div) Time Lines at: 0.50 sec intervals



Fourier Analysis (Amplitude Spectrum)

